CrossMark

Efficient evaluation of the material response of tissues reinforced by statistically oriented fibres

Kotaybah Hashlamoun, Alfio Grillo and Salvatore Federico

Abstract. For several classes of soft biological tissues, modelling complexity is in part due to the arrangement of the collagen fibres. In general, the arrangement of the fibres can be described by defining, at each point in the tissue, the structure tensor (i.e. the tensor product of the unit vector of the local fibre arrangement by itself) and a probability distribution of orientation. In this approach, assuming that the fibres do not interact with each other, the overall contribution of the collagen fibres to a given mechanical property of the tissue can be estimated by means of an averaging integral of the constitutive function describing the mechanical property at study over the set of all possible directions in space. Except for the particular case of fibre constitutive functions that are polynomial in the transversely isotropic invariants of the deformation, the averaging integral cannot be evaluated directly, in a single calculation because, in general, the integrand depends both on deformation and on fibre orientation in a non-separable way. The problem is thus, in a sense, analogous to that of solving the integral of a function of two variables, which cannot be split up into the product of two functions, each depending only on one of the variables. Although numerical schemes can be used to evaluate the integral at each deformation increment, this is computationally expensive. With the purpose of containing computational costs, this work proposes approximation methods that are based on the direct integrability of polynomial functions and that do not require the step-by-step evaluation of the averaging integrals. Three different methods are proposed: (a) a Taylor expansion of the fibre constitutive function in the transversely isotropic invariants of the deformation; (b) a Taylor expansion of the fibre constitutive function in the structure tensor; (c) for the case of a fibre constitutive function having a polynomial argument, an approximation in which the directional average of the constitutive function is replaced by the constitutive function evaluated at the directional average of the argument. Each of the proposed methods approximates the averaged constitutive function in such a way that it is multiplicatively decomposed into the product of a function of the deformation only and a function of the structure tensors only. In order to assess the accuracy of these methods, we evaluate the constitutive functions of the elastic potential and the Cauchy stress, for a biaxial test, under different conditions, i.e. different fibre distributions and different ratios of the nominal strains in the two directions. The results are then compared against those obtained for an averaging method available in the literature, as well as against the integration made at each increment of deformation.

Mathematics Subject Classification. 74-XX · 15-XX · 41-XX.

Keywords. Biological tissue · Collagen · Fibre-reinforced · Structure tensor · Fabric tensor · Averaging · Finite element method · Continuum mechanics · Elasticity.

1. Introduction

Soft biological tissues can be seen as highly complex fibre-reinforced materials [1]. The solid phase can be represented by a mixture of an isotropic matrix and transversely isotropic fibres. The spatial arrangement of the fibres largely defines the anisotropy and inhomogeneity of the tissue (e.g. [2,3]). In some tissues, the fibres can be thought of as being arranged in a finite number of families, each family being determined by the common direction of the fibres belonging to it. For instance, tissues typically modelled with a single

fibre family are ligaments and tendons [4], and tissues with two fibre families are blood vessels [5,6] and the atrium of the heart [7,8].

However, the fibres usually have some dispersion with respect to the dominant direction(s) (e.g. [6]). Moreover, there are tissues in which the dominant direction changes with location within the tissue or in which a dominant direction cannot be clearly defined. A prime example is articular cartilage, in which the fibre orientation varies along the depth of the tissue, from parallel to the surface in the superficial zone, to random in the middle zone (no dominant direction), to aligned to the depth direction in the deep zone [9,10]. Whenever one wishes to consider the dispersion about the dominant direction(s) or tissues with more complex fibre orientations, it is necessary to describe the arrangement of the fibres by means of an infinite number of statistically oriented fibres, which requires the use of an orientation probability distribution.

Orientation probability distributions in soft tissue biomechanics were first used by Lanir [11] and later adopted by several researchers (e.g. [6,12–14]). Similar techniques were independently developed in the context of composite materials with inclusions [15,16] and were subsequently transferred to biomechanical problems such as the determination of the overall elastic properties or the overall permeability of soft tissues. These models were extended to the case of large deformations, at first for the elasticity alone [17] and then for both elasticity and permeability [18]. Here, we shall use the notation and concepts developed in these previous works.

For an extensive physical quantity, such as mass, momentum, energy, the overall extent q of the quantity associated with the mixture as a whole is obtained as the weighted sum

$$q = \sum_{\alpha} \phi_{\alpha} \, q_{\alpha}, \tag{1}$$

where q_{α} is the value of the quantity in the constituent α and ϕ_{α} is the volumetric fraction of the constituent α. For lack of better knowledge, this *rule-of-mixture* can be extended also to quantities, such as the permeability, whose overall value may or may not be a linear combination as in Eq. (1). We are interested in mixtures including one or more fibre families, each having statistical orientation. The fibres in each family share the same properties but have different orientations, described by a probability distribution. Therefore, we think of each fibre family as an infinity of fibres and evaluate its overall contribution by means of an integral over all directions in space. The overall contribution of each fibre family to a certain physical quantity, given by the averaging integral of the quantity, is called *fibre ensemble*.

The method proposed in [6], which we call GOH method (Gasser–Ogden–Holzapfel method), accounts for the overall effect of each family of statistically oriented fibres by means of the directional average of the material structure tensor (the tensor product of the unit vector representing the material fibre direction by itself). In their approach to the overall elastic properties of the arterial wall, after having defined a fibre elastic potential as a function of the structure tensor of a given direction, Gasser et al. [6] replaced the structure tensor by its directional average. The rule-of-mixture method gives the same results of the GOH method whenever the material property to be averaged is an affine function (i.e. a constant plus a linear function) in the structure tensor [17]. The GOH method has the advantage of requiring one single integration, directly. Indeed, once the probability distribution is known, the directional average of the structure tensor is a given tensor that has to be evaluated only once and then used in all subsequent calculations. This makes the finite element (FE) implementation of the GOH method quite straightforward and, indeed, the GOH method is available in the material libraries of the commercially available software ABAQUS (Dassault Systèmes, Vélizy-Villacoublay, France).

In general, in the FE implementation of our rule-of-mixture method, the fibre ensemble (averaging integral of a certain physical quantity) must be calculated at each increment of deformation [17,19]. This is because of the coupled dependence of the integrand from *both* the structure tensor *and* the deformation.

Although sometimes fairly expensive from the computational point of view, an efficient numerical implementation of this method has been proposed [20], based on the use of spherical t-designs [21], in which the surface of the unit sphere is discretised into a suitable set of points, and the integral is evaluated as a summation on the discretised set of points. We recall that, since the oriented segment joining the centre of the unit sphere with a given point on its surface defines univocally a direction in space, the integration over the spherical surface can be made equivalent to integrating over all directions in space. Other numerical methods for finding the integration points on the surface of the sphere could be used (e.g. [22–24]), and a description of some of these methods can be found in [25]. However, a single, direct integration is possible whenever the integrand is a *separable function* of the deformation and the structure tensor, as is the case for *tensor-power polynomial* functions of the structure tensor (the definition of *tensor-power polynomial* is given later, in Sect. 2.3). We note that the GOH method is obtained in the instance of a tensor-power polynomial of degree one, which is an affine function of the structure tensor.

In this work, based on the direct integrability of polynomial functions, we introduce and compare three possible direct methods of approximation of the averaging integrals, with the purpose of estimating their accuracy and establishing the ranges within which they perform as alternative options to step-by-step integration criteria, while being computationally cheaper. We refer to these three methods as:

1. INEX (*Invariant Expansion*): the function to be averaged is viewed as a function of the invariants of the deformation that include the structure tensor, and then expanded in Taylor series about the values of the invariants in the reference configuration; then, the resulting polynomial is integrated;
2. STEX (*Structure Tensor Expansion*): the function to be averaged is expanded in Taylor series about the structure tensor of a convenient direction, and the resulting (tensor-power) polynomial is integrated;
3. PARG (*Polynomial Argument*): the function to be averaged is given by some function of an argument that is a (tensor-power) polynomial in the structure tensor, and the average is taken of the polynomial rather than of the whole function; in other words, the average is taken of the "outermost" argument that can be written as a (tensor-power) polynomial in the structure tensor.

These three methods are also compared with methods available in the literature:

4. GOH (*Gasser–Ogden–Holzapfel*): the model proposed by Gasser et al. [6]; the GOH method can be seen as the extreme of our PARG method, in which the "innermost" argument is averaged: the structure tensor;
5. FESD (*Fibre Ensemble with Spherical Designs*): the step-by-step integration of the fibre ensemble of a certain physical quantity performed with the method of the spherical t-designs [20,26].

The comparison is made based on a benchmark test in the context of elasticity, namely a biaxial tension test of a fibre-reinforced tissue sample, and the limitations of each methods are discussed.

2. Theoretical background

We refer the reader to the Appendix, where we briefly review the fairly standard continuum mechanics notation that we use (Appendix A), recall the definitions of the invariants of the deformation for the cases of isotropy and transverse isotropy (Appendix B), as well as some basic relations in nonlinear hyperelasticity (Appendix C), which will serve as our example of application of the averaging methods proposed in Sect. 3.

The notation follows that in a previous work [19], with a few small exceptions that allow for a lighter notation. The reference configuration of a body is denoted $\mathcal{B}$ (rather than $\mathcal{B}_R$), the referential volumetric fraction of constituent α of a mixture is denoted Φ_α (rather than $\phi_{\alpha R}$), and the referential probability distribution of orientation of the fibres is denoted Ψ (rather than ψ).

In this section, we first recall the volumetric–distortional decomposition of the deformation, which we use for a purpose different than the usual one (quasi-incompressible materials) and introduce some definitions that are useful for the objectives of this work. Then, we introduce some important definitions in tensor algebra and elucidate the averaging method based on the rule of mixtures that we employ in this work, and that gives rise to what we call the fibre ensemble. Finally, we recall the method by Gasser et al. [6] (GOH method), to which we compare our results.

2.1. The volumetric–distortional decomposition of the deformation

The volumetric–distortional decomposition of the deformation gradient $\boldsymbol{F}$ [27–29] is often employed in the treatment of quasi-incompressible materials. However, we shall use it for a different purpose, as outlined in Sect. 3.1. The deformation gradient tensor $\boldsymbol{F}$ can be decomposed into its volumetric and distortional (or isochoric) part, $\boldsymbol{F} = J^{1/3}\bar{\boldsymbol{F}}$. We refer to $\bar{\boldsymbol{F}}$ as to the distortional (or isochoric) part of $\boldsymbol{F}$, since, by construction, it is characterised by having a unitary determinant, i.e. $\det \bar{\boldsymbol{F}} = 1$. Consistently, we decompose the right Cauchy-Green deformation tensor as $\boldsymbol{C} = J^{2/3}\bar{\boldsymbol{C}}$, where the isochoric part of $\boldsymbol{C}$ is given by $\bar{\boldsymbol{C}} = \bar{\boldsymbol{F}}^{\mathrm{T}}.\bar{\boldsymbol{F}}$ and satisfies the equality $\det \bar{\boldsymbol{C}} = 1$.

2.2. Some important definitions in tensor algebra

Here, we introduce some definitions for the case of material tensors but, naturally, these are analogous for the case of spatial tensors. We indicate the full contraction of a material "contravariant" tensor $\mathbb{T}$ and a material "covariant" tensor $\mathbb{Z}$ of the same order r by means of the bra-ket notation $\langle \mathbb{T}|\mathbb{Z}\rangle = \mathrm{T}^{A_1\cdots A_r}\mathrm{Z}_{A_1\ldots A_r}$. Note that the bra-ket notation can be used symmetrically, i.e. $\langle \mathbb{T}|\mathbb{Z}\rangle = \langle \mathbb{Z}|\mathbb{T}\rangle$. For the particular case of second-order tensors, we can alternatively write $\boldsymbol{T} : \boldsymbol{Z} \equiv \langle \boldsymbol{T}|\boldsymbol{Z}\rangle = T^{AB}Z_{AB}$ and we call $\boldsymbol{T} : \boldsymbol{Z}$ the double contraction of $\boldsymbol{T}$ and $\boldsymbol{Z}$.

Given any n material tensors $\mathbb{A}_1, \ldots, \mathbb{A}_n$ of the same "contravariant" order r, "covariant" order s and overall order $r + s$, the *major-symmetric part* of the $n(r + s)$-th-order tensor

$$\mathbb{T} = \mathbb{A}_1 \otimes \cdots \otimes \mathbb{A}_n \tag{2}$$

is given by

$$\mathrm{msym}(\mathbb{T}) = \frac{1}{n!} \sum_{\sigma \in \mathfrak{S}_n} \mathbb{A}_{\sigma_1} \otimes \cdots \otimes \mathbb{A}_{\sigma_n}, \tag{3}$$

where each $\sigma = \{\sigma_1, \ldots, \sigma_n\}$ is one of all the $n!$ possible permutations $\mathfrak{S}_n$ of $\{1, \ldots, n\}$. Note that, if the tensors $\mathbb{A}_i$ are of the first order (i.e. they are all vectors $\boldsymbol{W}_i$ or all covectors $\boldsymbol{\Pi}_i$), then the major-symmetric part of $\mathbb{T}$ coincides with its symmetric part.

For any material tensor $\mathbb{A}$ (of any "contravariant" order r, "covariant" order s, and overall order $r+s$), its n-th tensor power is defined as the $n(r + s)$-th-order tensor

$$\mathbb{A}^{\otimes n} = \underbrace{\mathbb{A} \otimes \cdots \otimes \mathbb{A}}_{n \text{ times}}, \tag{4}$$

and, by convention, we set $\mathbb{A}^{\otimes 1} = \mathbb{A}$ and $\mathbb{A}^{\otimes 0} = 1 \in \mathbb{R}$. Given two tensors $\mathbb{A}, \mathbb{B}$ (of the same "contravariant" order r, "covariant" order s, and overall order $r + s$), the binomial tensor power $(\mathbb{A} + \mathbb{B})^{\otimes n}$ is given by the generalised Newton's formula

$$(\mathbb{A} + \mathbb{B})^{\otimes n} = \sum_{k=0}^{n} \left[\binom{n}{k} \mathrm{msym}\left(\mathbb{A}^{\otimes(n-k)} \otimes \mathbb{B}^{\otimes k}\right) \right], \tag{5}$$

where we recall that $\binom{n}{k}$ is the binomial coefficient $\binom{n}{k} = n!/(k!(n - k)!)$.

2.3. Materials with statistically oriented fibres

Let $\mathcal{F}$ be a generic physical quantity associated with a fibre-reinforced material, comprised of an isotropic matrix and anisotropic statistically oriented fibres. The considered quantity may be either a thermo-mechanical variable, such as stress, or a material property, such as stiffness or permeability. The mixture of matrix and fibres is assumed to be constrained, i.e. the matrix and fibres attain the same motion, with the same velocity $\boldsymbol{v}$ and the same deformation gradient $\boldsymbol{F}$. For the sake of simplicity, we limit ourselves to the case of a single family of statistically oriented fibres. The orientation of the fibres is described by the probability $\Psi(\boldsymbol{M})$ to find a fibre in a given referential direction $\boldsymbol{M}$ in the material unit sphere $\mathbb{S}^2\mathcal{B} = \{\boldsymbol{M} : \|\boldsymbol{M}\| = 1\}$. The probability density function Ψ is assumed to be invariant under the transformation $\boldsymbol{M} \mapsto -\boldsymbol{M}$ and normalised to one over the sphere, i.e. [30,31],

$$\Psi(-\boldsymbol{M}) = \Psi(\boldsymbol{M}), \qquad \int_{\mathbb{S}^2\mathcal{B}} \Psi(\boldsymbol{M}) = 1. \tag{6}$$

Note that we shall omit writing the "area element" or, more properly, the *area two-form* [32,33] "dS" in all surface integrals. If Φ_0 and Φ_1 are the referential volumetric fractions of the matrix and the fibres, respectively, the physical quantity $\mathcal{F}$ can be written, in the reference configuration, with the rule-of-mixture expression

$$\mathcal{F} = \hat{\mathcal{F}}(\boldsymbol{C}, \Psi) = \Phi_0 \, \hat{\mathcal{F}}_0(\boldsymbol{C}) + \Phi_1 \int_{\mathbb{S}^2\mathcal{B}} \Psi(\boldsymbol{M}) \hat{\mathcal{F}}_1(\boldsymbol{C}, \boldsymbol{A}), \tag{7}$$

where $\boldsymbol{A} = \boldsymbol{M} \otimes \boldsymbol{M}$ is the structure tensor, $\hat{\mathcal{F}}$ is the constitutive function of $\mathcal{F}$, $\hat{\mathcal{F}}_0$ is the isotropic constitutive function of quantity $\mathcal{F}_0$ in the matrix, and $\hat{\mathcal{F}}_1$ is the anisotropic constitutive function of quantity $\mathcal{F}_1$ in the fibres. The integral

$$\mathcal{F}_e = \hat{\mathcal{F}}_e(\boldsymbol{C}, \Psi) = \int_{\mathbb{S}^2\mathcal{B}} \Psi(\boldsymbol{M}) \hat{\mathcal{F}}_1(\boldsymbol{C}, \boldsymbol{A}), \tag{8}$$

called the *fibre ensemble of* $\mathcal{F}_1$ [18,19], accounts for the effect of the fibres and had initially been introduced for the case of the elastic potential [17].

In general, it is not possible to factorise the deformation $\boldsymbol{C}$ out of the integral, and therefore the fibre ensemble cannot be calculated directly, but must be evaluated at each increment of deformation. This has been done [20] by means of the method of the spherical t-designs [21,34], i.e. a set of N points $\{\boldsymbol{M}^{(1)}, \ldots, \boldsymbol{M}^{(N)}\}$ in the material unit sphere $\mathbb{S}^2\mathcal{B}$ such that, for polynomials $\mathcal{P}$ of degree $k \leq t$,

$$\int_{\mathbb{S}^2\mathcal{B}} \mathcal{P}(\boldsymbol{M}) = \frac{4\pi}{N} \sum_{r=1}^{N} \mathcal{P}(\boldsymbol{M}^{(r)}), \tag{9}$$

where 4π is the (surface) measure of the unit sphere $\mathbb{S}^2\mathcal{B}$. As mentioned in the Introduction, we shall denote the numerical integration of the rule-of-mixture expression of the fibre ensemble of Eq. (8), performed with the method of the spherical designs, by the acronym FESD.

It is crucial to remark that a single, direct integration is possible when the constitutive function $\hat{\mathcal{F}}_1$ is a *separable* function of the structure tensor $\boldsymbol{A}$ and the deformation $\boldsymbol{C}$. For a (scalar) constitutive function $\hat{\mathcal{F}}_1$, the most common case of separable function is a *tensor-power polynomial* in the structure tensor $\boldsymbol{A}$ [19], of the type

$$\hat{\mathcal{F}}_1(\boldsymbol{C}, \boldsymbol{A}) = a \left[q_0(\boldsymbol{C}) + \sum_{p=1}^{n} \langle \mathbb{Q}_p(\boldsymbol{C}) | \boldsymbol{A}^{\otimes p} \rangle \right], \tag{10}$$

where a is a material constant with units of $\mathcal{F}_1$, $q_0(\boldsymbol{C})$ is a non-dimensional scalar function of the deformation and the non-dimensional "covariant" tensor functions $\mathbb{Q}_p$ are such that $\mathbb{Q}_p(\boldsymbol{C})$ is a tensor

of order $2p$, which contracts with the "contravariant" tensor-power $\boldsymbol{A}^{\otimes p}$, which is the tensor of order $2p$ defined by

$$\boldsymbol{A}^{\otimes p} = \underbrace{\boldsymbol{A} \otimes \cdots \otimes \boldsymbol{A}}_{p \text{ times}}. \tag{11}$$

Note that the tensors $\mathbb{Q}_p(\boldsymbol{C})$ and $\boldsymbol{A}^{\otimes p}$ are fully "covariant" and fully "contravariant", respectively, which justifies the bra-ket notation, $\langle \cdot \, | \, \cdot \rangle$. For the constitutive function in Eq. (10), it is possible to exploit the linearity of the integration operator and to factorise the deformation out of each resulting integral, so that the fibre ensemble of Eq. (8) becomes [19]

$$\mathcal{F}_e = \hat{\mathcal{F}}_e(\boldsymbol{C}, \Psi) = a \left[q_0(\boldsymbol{C}) + \sum_{p=1}^{n} \langle \mathbb{Q}_p(\boldsymbol{C}) | \mathbb{H}_p \rangle \right], \tag{12}$$

where we define the averaged structure tensor of order $2p$ as [19,30,31,35]

$$\mathbb{H}_p = \int\limits_{\mathbb{S}^2 \mathcal{B}} \Psi(\boldsymbol{M}) \, \boldsymbol{A}^{\otimes p}. \tag{13}$$

Therefore, an analytical form of the fibre ensemble can be obtained as a function of the deformation $\boldsymbol{C}$ and can be introduced directly into a finite element implementation, without the need to calculate an integral at each increment of deformation.

We shall exploit the property of direct integrability of polynomial constitutive functions to propose our integration methods in Sect. 3.

Remark. We refer to the constitutive function of Eq. (10) as to a tensor-power polynomial because the *tensor power* $\boldsymbol{A}^{\otimes p}$ is involved, rather than the regular power $\boldsymbol{A}^p$. Indeed, because of the *idempotence* of $\boldsymbol{A}$ [36,37], the regular power would lead to the trivial result $\boldsymbol{A}^p = \boldsymbol{A}$, which means that any (regular) polynomial of the N-th order in $\boldsymbol{A}$ would reduce to an affine function in $\boldsymbol{A}$. The idempotence of $\boldsymbol{A}$ can be shown in components:

$$(\boldsymbol{A}^2)^{AD} = A^{AB} G_{BC} A^{CD} = M^A M^B G_{BC} M^C M^D = M^A M^D = A^{AD}. \tag{14}$$

Furthermore, we note that, for a second-order tensor, whereas the regular power is an *internal* operation, the tensor power is an *external* operation, in so far as its result is a tensor of different order than the original one. A particularly interesting case occurs when the $2p$-th-order tensor $\mathbb{Q}_p(\boldsymbol{C})$ can be written as the tensor product of p tensors of order two. An even more peculiar situation occurs when it holds that $\mathbb{Q}_p(\boldsymbol{C}) = q_p(\boldsymbol{C}) \, \boldsymbol{C}^{\otimes p}$, for every $p \in \{1, \ldots, N\}$, with $q_p(\boldsymbol{C})$ being a suitable scalar-valued function of $\boldsymbol{C}$, so that Eq. (10) becomes

$$\hat{\mathcal{F}}_1(\boldsymbol{C}, \boldsymbol{A}) = a \left[q_0(\boldsymbol{C}) + \sum_{p=1}^{n} q_p(\boldsymbol{C}) \, \langle \boldsymbol{C}^{\otimes p} | \boldsymbol{A}^{\otimes p} \rangle \right]. \tag{15}$$

Because of the identity

$$I_4^p = (\boldsymbol{C} : \boldsymbol{A})^p = \langle \boldsymbol{C} | \boldsymbol{A} \rangle^p = \left\langle \boldsymbol{C}^{\otimes p} \big| \boldsymbol{A}^{\otimes p} \right\rangle, \tag{16}$$

expression (15) becomes a polynomial of degree N in the fourth invariant $I_4 = \langle \boldsymbol{C} | \boldsymbol{A} \rangle = \boldsymbol{C} : \boldsymbol{A}$, i.e.

$$\hat{\mathcal{F}}_1(\boldsymbol{C}, \boldsymbol{A}) = \check{\mathcal{F}}_1(I_4) = q_0(\boldsymbol{C}) + \sum_{p=1}^{N} q_p(\boldsymbol{C}) \, I_4^p. \tag{17}$$

2.4. Averaged structure tensors $\mathbb{H}_p$ of order $2p$

To the best of our knowledge, the generalised structure tensors that we denote $\mathbb{H}_p$ in Eq. (13) were first introduced by Kanatani [30], who actually called "fabric tensors" the *deviatoric* parts of the $\mathbb{H}_p$, with some normalisation constants [cf., in [30], Equation (3.4), which corresponds exactly to the definition of $\mathbb{H}_p$, and Equation (3.3), which defines Kanatani's "fabric tensors"]. Advani and Tucker [31] noted that all averaged structure tensors of order smaller than $p \geq 2$ can be found from $\mathbb{H}_p$ by contracting pairs of its indices (which, in our formalism, requires the use of the metric tensor), as it can be shown, e.g. in components. Our group first employed the tensors $\mathbb{H}_p$ only recently [19] and, regretfully, we were unaware of the works by Kanatani [30] and Advani and Tucker [31] at that time. For $p = 1$, the averaged tensor in Eq. (13) coincides with the second-order tensor given by the average of the structure tensor $\boldsymbol{A}$,

$$\boldsymbol{H} = \int\limits_{\mathbb{S}^2\mathcal{B}} \Psi(\boldsymbol{M})\,\boldsymbol{A}, \tag{18}$$

which Gasser et al. [6] called "generalised structure tensor" and used as the basis of their averaging method (see Sect. 2.5). In the following, we will generally use the identification $\mathbb{H}_1 \equiv \boldsymbol{H}$, except in sums over p involving the tensors $\mathbb{H}_p$ of order $2p$. To our knowledge, prior to this work, the fourth-order averaged structure tensor $\mathbb{H}_2$ was used in biomechanics by Vasta et al. [38] and Gizzi et al. [39], who called it simply $\mathbb{H}$.

2.5. The Gasser–Ogden–Holzapfel method (GOH)

The method proposed by Gasser et al. [6], thereby called GOH method, allows for a single, direct integration, and we describe it here in our notation. Gasser et al. [6] proposed to evaluate the overall effect of the fibres on a physical quantity $\mathcal{F}$ by replacing the structure tensor $\boldsymbol{A}$ in the fibre function $\mathcal{F}_1 = \hat{\mathcal{F}}_1(\boldsymbol{C}, \boldsymbol{A})$ by means of its directional average $\boldsymbol{H}$ introduced in Eq. (18), to obtain

$$\mathcal{F}_{\mathrm{GOH}} = \hat{\mathcal{F}}_{\mathrm{GOH}}(\boldsymbol{C}, \Psi) = \hat{\mathcal{F}}_1(\boldsymbol{C}, \boldsymbol{H}), \tag{19}$$

which they used in Eq. (7) in place of our fibre ensemble $\hat{\mathcal{F}}_e$ of Eq. (8). When $\hat{\mathcal{F}}_1$ is affine in the structure tensor $\boldsymbol{A}$, i.e. it is a (tensor-power) polynomial of degree one in $\boldsymbol{A}$,

$$\hat{\mathcal{F}}_1(\boldsymbol{C}, \boldsymbol{A}) = a\,[q_0(\boldsymbol{C}) + \boldsymbol{Q}(\boldsymbol{C}) : \boldsymbol{A}], \tag{20}$$

where a is a constant, q_0 is a scalar function of $\boldsymbol{C}$, and $\boldsymbol{Q}$ is a second-order "covariant" tensor-valued function of $\boldsymbol{C}$, we have

$$
\begin{aligned}
\hat{\mathcal{F}}_e(\boldsymbol{C}, \Psi) &= \int\limits_{\mathbb{S}^2\mathcal{B}} \Psi(\boldsymbol{M})\,\hat{\mathcal{F}}_1(\boldsymbol{C}, \boldsymbol{A}) = \int\limits_{\mathbb{S}^2\mathcal{B}} \Psi(\boldsymbol{M})\,a\,[q_0(\boldsymbol{C}) + \boldsymbol{Q}(\boldsymbol{C}) : \boldsymbol{A}] \\
&= a\left[q_0(\boldsymbol{C}) + \boldsymbol{Q}(\boldsymbol{C}) : \left(\int\limits_{\mathbb{S}^2\mathcal{B}} \Psi(\boldsymbol{M})\boldsymbol{A}\right)\right] = a\,[q_0(\boldsymbol{C}) + \boldsymbol{Q}(\boldsymbol{C}) : \boldsymbol{H}] \\
&= \hat{\mathcal{F}}_1(\boldsymbol{C}, \boldsymbol{H}) = \hat{\mathcal{F}}_{\mathrm{GOH}}(\boldsymbol{C}, \Psi),
\end{aligned}
\tag{21}
$$

i.e. the rule-of-mixture method coincides with the GOH method [17].

3. Approximation of the fibre ensemble

Here we introduce three methods that provide analytical approximations of the fibre ensemble (8), all based on the fact that, for a fibre function $\hat{\mathcal{F}}_1$ that is a tensor-power polynomial in the structure tensor, a

single, direct integration is possible [19]. Two of the proposed methods are based on the Taylor expansion of the fibre function $\hat{\mathcal{F}}_1$, in order to obtain polynomial functions in the structure tensor $\boldsymbol{A}$. In the first method, we expand in the transversely isotropic invariants, which are linear functions of $\boldsymbol{A}$ (see Eq. (72)). In the second method, we expand in the structure tensor $\boldsymbol{A}$. In the third method, in a fashion similar to that of the GOH method [6], for the case of a fibre function $\hat{\mathcal{F}}_1$ that is a function of a tensor-power polynomial $\mathcal{P}(\boldsymbol{A})$, we replace the fibre ensemble by the same function evaluated at the directional average of $\mathcal{P}(\boldsymbol{A})$, which can be calculated directly.

3.1. Taylor expansion in the invariants (INEX)

Let $\check{\mathcal{F}}_1(I_1, I_2, I_3, I_4, I_5) = \hat{\mathcal{F}}_1(\boldsymbol{C}, \boldsymbol{A})$ be the fibre constitutive function written as a function of the five transversely isotropic invariants (when looking at a single direction $\boldsymbol{M}$, the symmetry is naturally that of transverse isotropy). For the sake of a lighter notation, let us omit writing the three isotropic invariants I_1, I_2, I_3 among the arguments of $\check{\mathcal{F}}_1$ and, for the sake of a simpler presentation, let us assume that $\check{\mathcal{F}}_1$ does not depend on the fifth invariant I_5. If I_5 were included, the derivation would be analogous, but lengthier, and the Taylor expansion formulae would require the introduction of the multi-index notation. Furthermore, we write $I_4 = J^{2/3}\bar{I}_4$, i.e. we express I_4 in terms of its purely distortional counterpart $\bar{I}_4$. Therefore, let us write the fibre quantity $\mathcal{F}_1$ as a constitutive function of J and $\bar{I}_4$, i.e.

$$\mathcal{F}_1 = \hat{\mathcal{F}}_1(\boldsymbol{C}, \boldsymbol{A}) = \check{\mathcal{F}}_1(J, \bar{I}_4). \tag{22}$$

We remark that, although we omitted indicating explicitly the dependence of $\check{\mathcal{F}}_1$ on $I_3 = J^2$, in the sequel we express $\check{\mathcal{F}}_1$ as a function of $\bar{I}_4$ *and* J in order to emphasise that J is used to express I_4 as $J^{2/3}\bar{I}_4$. We also remark that we are *not* decomposing I_4 into its volumetric and distortional parts in order to impose incompressibility, which is the most common case in which one uses the volumetric–distortional decomposition, but because it serves our purpose of a Taylor expansion at a point of zero (distortional) deformation, as it will be explained later.

For a given $\boldsymbol{C} = J^{2/3}\bar{\boldsymbol{C}}$, it is fairly straightforward to prove that the admissible values of I_4 and $\bar{I}_4$ belong to the closed intervals $\Lambda(\boldsymbol{C}) = [\lambda_{\min}^2, \lambda_{\max}^2]$ and $\Lambda(\bar{\boldsymbol{C}}) = [\bar{\lambda}_{\min}^2, \bar{\lambda}_{\max}^2]$, respectively, where $\lambda_{\min}^2$ and $\lambda_{\max}^2$ are the minimum and maximum eigenvalue of $\boldsymbol{C}$, and $\bar{\lambda}_{\min}^2$ and $\bar{\lambda}_{\max}^2$ are those of $\bar{\boldsymbol{C}}$ (see Appendix D for both an analytical and graphical proof). Note that, in the undeformed configuration, for which $\boldsymbol{C} = \bar{\boldsymbol{C}} = \boldsymbol{G}$ (where the metric tensor $\boldsymbol{G}$ serves as the "covariant" identity tensor), the intervals $\Lambda(\boldsymbol{C})$ and $\Lambda(\bar{\boldsymbol{C}})$ degenerate into the singleton $\Lambda(\boldsymbol{G}) = \{1\}$. We also remark that the admissible intervals of I_5 and $\bar{I}_5$ have the same form of those of I_4 and $\bar{I}_4$, except that the exponents 2 of the maximum and minimum stretches have to be replaced by exponents 4.

For our purposes, it is very important to note that it is *always* verified that $\bar{I}_{40} = 1 \in \Lambda(\bar{\boldsymbol{C}}) = [\bar{\lambda}_{\min}^2, \bar{\lambda}_{\max}^2]$. Indeed, the condition $\det \bar{\boldsymbol{C}} = 1$ implies that $\bar{\lambda}_{\min}^2 < 1$ and $\bar{\lambda}_{\max}^2 > 1$. Therefore, if $\check{\mathcal{F}}_1$ belongs to the space $C^n(\mathring{\Lambda}(\bar{\boldsymbol{C}}))$ of continuously differentiable functions up to order n in the open set $\mathring{\Lambda}(\bar{\boldsymbol{C}}) =]\bar{\lambda}_{\min}^2, \bar{\lambda}_{\max}^2[$ of the interior points of $\Lambda(\bar{\boldsymbol{C}})$, it is possible to approximate $\check{\mathcal{F}}_1$ by means of a Taylor expansion in the variable $\bar{I}_4$, about the value $\bar{I}_{40} = 1 \in \Lambda(\bar{\boldsymbol{C}})$. For this purpose, we invoke the Taylor's expansion formula of order n for $\check{\mathcal{F}}_1$, which reads

$$\check{\mathcal{F}}_1(J, \bar{I}_4) = \check{\mathcal{T}}_n(J, \bar{I}_4) + \check{\mathcal{R}}_n(J, \bar{I}_4) = \sum_{j=0}^{n} \frac{1}{j!} \frac{\partial^{(j)}\check{\mathcal{F}}_1}{\partial \bar{I}_4^{(j)}}(J, 1)[\bar{I}_4 - 1]^j + \check{\mathcal{R}}_n(J, \bar{I}_4), \tag{23}$$

where $\check{\mathcal{T}}_n(J, \bar{I}_4)$ is the Taylor polynomial of order n associated with $\check{\mathcal{F}}_1$ at $1 \in \mathring{\Lambda}(\bar{\boldsymbol{C}})$. If $\check{\mathcal{F}}_1$ is differentiable $n+1$ times in $\mathring{\Lambda}(\bar{\boldsymbol{C}}) \setminus \{1\}$, the remainder $\check{\mathcal{R}}_n(\bar{I}_4)$ can be given in Lagrange's form as

$$\check{\mathcal{R}}_n(J, \bar{I}_4) = \frac{1}{(n+1)!} \frac{\partial^{(n+1)}\check{\mathcal{F}}_1}{\partial \bar{I}_4^{(n+1)}}(J, \xi_{n+1})[\bar{I}_4 - 1]^{n+1}, \tag{24}$$

for some $\xi_{n+1} \in \mathring{\Lambda}(\boldsymbol{C})$ lying between 1 and $\bar{I}_4$ and depending on $\bar{I}_4$ as well as on the order n of the expansion.

We now exploit $\bar{I}_4 = \bar{\boldsymbol{C}} : \boldsymbol{A} = J^{-2/3}\boldsymbol{C} : \boldsymbol{A}$ and write the Taylor polynomial and the remainder as explicit functions of the structure tensor $\boldsymbol{A}$, i.e.

$$\check{\mathcal{T}}_n(J, \bar{I}_4) = \hat{\mathcal{T}}_n(\boldsymbol{C}, \boldsymbol{A}) = \sum_{j=0}^{n} \frac{1}{j!} \frac{\partial^{(j)}\check{\mathcal{F}}_1}{\partial \bar{I}_4^{(j)}}(J, 1)[J^{-2/3}\boldsymbol{C} : \boldsymbol{A} - 1]^j, \tag{25a}$$

$$\check{\mathcal{R}}_n(J, \bar{I}_4) = \hat{\mathcal{R}}_n(\boldsymbol{C}, \boldsymbol{A}) = \frac{1}{(n+1)!} \frac{\partial^{(n+1)}\check{\mathcal{F}}_1}{\partial \bar{I}_4^{(n+1)}}(J, \xi_{n+1})[J^{-2/3}\boldsymbol{C} : \boldsymbol{A} - 1]^{n+1}, \tag{25b}$$

which give

$$\hat{\mathcal{F}}_1(\boldsymbol{C}, \boldsymbol{A}) = \hat{\mathcal{T}}_n(\boldsymbol{C}, \boldsymbol{A}) + \hat{\mathcal{R}}_n(\boldsymbol{C}, \boldsymbol{A}). \tag{26}$$

Then, we multiply both sides of Eq. (26) by the probability distribution $\Psi(\boldsymbol{M})$, integrate over the material sphere $\mathbb{S}^2\mathcal{B}$ and obtain

$$\mathcal{F}_e = \mathcal{G}_n + \mathcal{E}_n, \tag{27}$$

where $\mathcal{F}_e$ is the fibre ensemble of Eq. (8), and

$$\mathcal{G}_n = \int_{\mathbb{S}^2\mathcal{B}} \Psi(\boldsymbol{M}) \hat{\mathcal{T}}_n(\boldsymbol{C}, \boldsymbol{A}), \tag{28a}$$

$$\mathcal{E}_n = \int_{\mathbb{S}^2\mathcal{B}} \Psi(\boldsymbol{M}) \hat{\mathcal{R}}_n(\boldsymbol{C}, \boldsymbol{A}), \tag{28b}$$

are the n-th-order approximation of $\mathcal{F}_e$ and the corresponding error $\mathcal{E}_n$, which is entirely defined by the difference $\mathcal{E}_n := \mathcal{F}_e - \mathcal{G}_n$. Equation (28a) defines the sequence $\{\mathcal{G}_n\}_{n\in\mathbb{N}}$, in which $\mathcal{G}_n$ is given by

$$\mathcal{G}_n = \hat{\mathcal{G}}_n(\boldsymbol{C}, \Psi) = \sum_{j=0}^{n} \frac{1}{j!} \frac{\partial^{(j)}\check{\mathcal{F}}_1}{\partial \bar{I}_4^{(j)}}(J, 1) \int_{\mathbb{S}^2\mathcal{B}} \Psi(\boldsymbol{M}) [J^{-2/3}\boldsymbol{C} : \boldsymbol{A} - 1]^j$$

$$= \sum_{j=0}^{n} \frac{1}{j!} \frac{\partial^{(j)}\check{\mathcal{F}}_1}{\partial \bar{I}_4^{(j)}}(J, 1) \sum_{k=0}^{j} \binom{j}{k} (-1)^k (J^{-2/3})^{j-k} \int_{\mathbb{S}^2\mathcal{B}} \Psi(\boldsymbol{M}) [\boldsymbol{C} : \boldsymbol{A}]^{j-k}. \tag{29}$$

The Cauchy-Green deformation tensor $\boldsymbol{C}$ can be factorised out of the integral sign in (29) by using the identity (16), from which

$$\int_{\mathbb{S}^2\mathcal{B}} \Psi(\boldsymbol{M}) [\boldsymbol{C} : \boldsymbol{A}]^{j-k} = \left\langle \boldsymbol{C}^{\otimes(j-k)} \middle| \mathbb{H}_{j-k} \right\rangle. \tag{30}$$

By virtue of this result, the n-th-order approximation of $\mathcal{F}_e$ can be recast in the compact form

$$\mathcal{G}_n = \hat{\mathcal{G}}_n(\boldsymbol{C}, \Psi) = \sum_{j=0}^{n} \frac{1}{j!} \frac{\partial^{(j)}\check{\mathcal{F}}_1}{\partial \bar{I}_4^{(j)}}(J, 1) \sum_{k=0}^{j} \binom{j}{k} (-1)^k (J^{-2/3})^{j-k} \left\langle \boldsymbol{C}^{\otimes(j-k)} \middle| \mathbb{H}_{j-k} \right\rangle, \tag{31}$$

in which the deformation has been completely factorised with respect to directional averaging, the latter being accounted for by the averaged structure tensor of order $2(j-k)$, $\mathbb{H}_{j-k}$. To estimate the error, let us consider for simplicity the case in which $\mathcal{F}_1$ is a scalar constitutive function, so that its associated fibre ensemble, $\mathcal{F}_e$, and n-th-order approximation, $\mathcal{G}_n$, are scalars too. If the error $\mathcal{E}_n = \mathcal{F}_e - \mathcal{G}_n$ vanishes as n goes towards infinity, $\mathcal{F}_e$ can be represented exactly by the limit $\lim_{n\to\infty} \mathcal{G}_n$, in which case it holds that

$$\mathcal{F}_e = \lim_{n\to\infty} \mathcal{G}_n. \tag{32}$$

To estimate $\mathcal{E}_n$, we follow the theory of Taylor expansion formulae, and we infer that, if there exist positive constants L and Q, such that

$$\left| \frac{\partial^{n+1} \check{\mathcal{F}}_1}{\partial \bar{I}_4^{n+1}} (J, \bar{I}_4) \right| \le L \, Q^{n+1}, \quad \forall \, \bar{I}_4 \in \mathring{\Lambda}(\bar{\boldsymbol{C}}), \tag{33}$$

then it holds that

$$|\mathcal{E}_n| \le \int_{\mathbb{S}^2 \mathcal{B}} \Psi(\boldsymbol{M}) \left| \hat{\mathcal{R}}_n(\boldsymbol{C}, \boldsymbol{A}) \right| \le L \frac{Q^{n+1}}{(n+1)!} \int_{\mathbb{S}^2 \mathcal{B}} \Psi(\boldsymbol{M}) |\bar{I}_4 - 1|^{n+1} \le L \frac{Q^{n+1}(\bar{\lambda}_{\max}^2 - \bar{\lambda}_{\min}^2)^{n+1}}{(n+1)!}. \tag{34}$$

Note that, in the case in which $\mathcal{F}_1$ is a tensor-valued constitutive quantity, the estimates (33) and (34) must be generalised by replacing the absolute value with an appropriate norm.

For a sufficiently high order n of the Taylor's expansion (23), we enforce the approximation

$$\mathcal{F}_e \simeq \mathcal{G}_n, \tag{35}$$

the accuracy of which increases when the absolute value of the error, $|\mathcal{E}_n|$, tends towards zero. For example, this is the case when $\bar{\lambda}_{\max}^2$ and $\bar{\lambda}_{\min}^2$ tend to be equal to each other.

Equations (27) and (35) constitute the INEX (Invariant Expansion) method and provide a polynomial approximation of the fibre ensemble $\hat{\mathcal{F}}_e$, *regardless* of the form of the orientation probability distribution Ψ. This is achieved by expanding the fibre constitutive function $\check{\mathcal{F}}_1(J, \cdot)$ about $\bar{I}_{40} = 1$, which rules out any dependence on a "privileged" direction $\boldsymbol{M}_0$. In order to clearly show this, let $\boldsymbol{M}_0$ be any direction, with the associated structure tensor $\boldsymbol{A}_0 = \boldsymbol{M}_0 \otimes \boldsymbol{M}_0$. Since $\bar{I}_{40} = \bar{\boldsymbol{C}} : \boldsymbol{A}_0$, when $\bar{\boldsymbol{C}} = \boldsymbol{G}$, we have that $\bar{I}_{40} = 1$, *for every* $\boldsymbol{M}_0$. Therefore, the INEX approximation is valid for *any* orientation distribution Ψ. This is in contrast with the STEX method presented in Sect. 3.2, which is based on the expansion about $\boldsymbol{A}_0 = \boldsymbol{M}_0 \otimes \boldsymbol{M}_0$, and is thus accurate *only* for orientation distributions Ψ with small dispersions about $\boldsymbol{M}_0$. We observed that the INEX method gave the best results for even orders of expansion.

3.2. Taylor expansion in the structure tensor (STEX)

Given a fibre function $\mathcal{F}_1 = \hat{\mathcal{F}}_1(\boldsymbol{C}, \boldsymbol{A})$ and a structure tensor $\boldsymbol{A}_0 = \boldsymbol{M}_0 \otimes \boldsymbol{M}_0$, if $\hat{\mathcal{F}}_1$ is of class C^n in a neighbourhood of $\boldsymbol{A}_0$, it is possible to use Taylor's expansion formula in $\boldsymbol{A}$ about $\boldsymbol{A}_0$,

$$\hat{\mathcal{F}}_1(\boldsymbol{C}, \boldsymbol{A}) = \hat{\mathcal{T}}_n(\boldsymbol{C}, \boldsymbol{A}) + \hat{\mathcal{R}}_n(\boldsymbol{C}, \boldsymbol{A}) = \sum_{j=0}^{n} \frac{1}{j!} \left\langle \left. \frac{\partial^{(j)} \hat{\mathcal{F}}_1}{\partial \boldsymbol{A}^{(j)}} (\boldsymbol{C}, \boldsymbol{A}_0) \right| (\boldsymbol{A} - \boldsymbol{A}_0)^{\otimes j} \right\rangle + \hat{\mathcal{R}}_n(\boldsymbol{C}, \boldsymbol{A}), \tag{36}$$

where, similarly to the case of the INEX method, $\hat{\mathcal{T}}_n(\boldsymbol{C}, \boldsymbol{A})$ is the Taylor polynomial of order n, and if $\hat{\mathcal{F}}_1$ is of class C^{n+1} in $\boldsymbol{A}$, the remainder $\hat{\mathcal{R}}_n(\boldsymbol{C}, \boldsymbol{A})$ can be expressed in Lagrange's form (we omit the details).

Multiplying both sides of Eq. (36) by the probability density Ψ and then integrating over the material sphere $\mathbb{S}^2 \mathcal{B}$, we obtain

$$\mathcal{F}_e = \mathcal{G}_n + \mathcal{E}_n, \tag{37}$$

where, analogously to the case of the INEX method, $\mathcal{F}_e$ is the fibre ensemble of Eq. (8), $\mathcal{G}_n$ is the n-th-order approximation of $\mathcal{F}_e$ and $\mathcal{E}_n$ is the n-th-order error, defined formally as in Eqs. (28a) and (28b). The term $\mathcal{G}_n$ of the sequence $\{\mathcal{G}_n\}_{n \in \mathbb{N}}$ is given by

$$\mathcal{G}_n = \hat{\mathcal{G}}_n(\boldsymbol{C}, \Psi) = \int_{\mathbb{S}^2 \mathcal{B}} \left[\Psi(\boldsymbol{M}) \sum_{j=0}^{n} \frac{1}{j!} \left\langle \frac{\partial^{(j)} \hat{\mathcal{F}}_1}{\partial \boldsymbol{A}^{(j)}}(\boldsymbol{C}, \boldsymbol{A}_0) \middle| (\boldsymbol{A} - \boldsymbol{A}_0)^{\otimes j} \right\rangle \right]$$

$$= \sum_{j=0}^{n} \frac{1}{j!} \left\langle \frac{\partial^{(j)} \hat{\mathcal{F}}_1}{\partial \boldsymbol{A}^{(j)}}(\boldsymbol{C}, \boldsymbol{A}_0) \middle| \int_{\mathbb{S}^2 \mathcal{B}} \Psi(\boldsymbol{M}) (\boldsymbol{A} - \boldsymbol{A}_0)^{\otimes j} \right\rangle. \tag{38}$$

Note that the integrals on the right-hand side of the bra-ket are independent of the deformation $\boldsymbol{C}$. Using the expression (5) of the binomial tensor power and the linearity of the integral operation, it is possible to write Eq. (38) in the form

$$\mathcal{F}_e \simeq \mathcal{G}_n = \hat{\mathcal{G}}_n(\boldsymbol{C}, \Psi) = \sum_{j=0}^{n} \frac{1}{j!} \left\langle \frac{\partial^{(j)} \hat{\mathcal{F}}_1}{\partial \boldsymbol{A}^{(j)}}(\boldsymbol{C}, \boldsymbol{A}_0) \middle| \sum_{k=0}^{j} \left[(-1)^k \binom{j}{k} \operatorname{msym}\left(\mathbb{H}_{j-k} \otimes \boldsymbol{A}_0^{\otimes k}\right) \right] \right\rangle, \tag{39}$$

which features the averaged structure tensors $\mathbb{H}_p$ of Eq. (13). Equations (37) and (39) yield an analytical approximation of the fibre potential $\mathcal{F}_e$ as a function of the deformation $\boldsymbol{C}$. It seems natural to expand about the structure tensor $\boldsymbol{A}_0 = \boldsymbol{M}_0 \otimes \boldsymbol{M}_0$ relative to the dominant direction $\boldsymbol{M}_0$ of the fibres, in which case the best results are obtained when the dispersion of the fibres about that direction is relatively small. We note that Vasta et al. [38] have in fact implemented what here we would call the STEX method of order 2, i.e. involving only $\mathbb{H}_1 \equiv \boldsymbol{H}$ and $\mathbb{H}_2$. Also in this case, the best results were obtained for even orders of expansion.

3.3. Polynomial argument method (PARG)

In this section, we consider a fibre function of the type

$$\mathcal{F}_1 = \hat{\mathcal{F}}_1(\boldsymbol{C}, \boldsymbol{A}) = \mathfrak{f}\left(\mathcal{P}(\boldsymbol{C}, \boldsymbol{A})\right), \tag{40}$$

where $\mathfrak{f}$ describes the physical quantity that has to be modelled (e.g. the elastic potential) and $\mathcal{P}(\boldsymbol{C}, \boldsymbol{A})$ is defined by the N-th degree *tensor-power polynomial*

$$\mathcal{P}(\boldsymbol{C}, \boldsymbol{A}) := q_0(\boldsymbol{C}) + \sum_{p=1}^{N} \langle \mathbb{Q}_p(\boldsymbol{C}) | \boldsymbol{A}^{\otimes p} \rangle, \tag{41}$$

in which, as in Eq. (10), q_0 and $\mathbb{Q}_p$ are, respectively, a non-dimensional scalar-valued function and a non-dimensional "covariant" tensor-valued function of order $2p$ of the right Cauchy-Green deformation tensor. We propose to approximate the fibre ensemble as

$$\mathcal{F}_e = \hat{\mathcal{F}}_e(\boldsymbol{C}, \Psi) = \int_{\mathbb{S}^2 \mathcal{B}} \Psi(\boldsymbol{M}) \mathfrak{f}\left(\mathcal{P}(\boldsymbol{C}, \boldsymbol{A})\right) \simeq \mathfrak{f}\left(\int_{\mathbb{S}^2 \mathcal{B}} \Psi(\boldsymbol{M}) \mathcal{P}(\boldsymbol{C}, \boldsymbol{A}) \right). \tag{42}$$

This approximation becomes exact if the operation of directional averaging commutes with the function $\mathfrak{f}$. This holds true, for example, when $\mathfrak{f}$ is a polynomial of degree M in $\mathcal{P}(\boldsymbol{C}, \boldsymbol{A})$, and $\mathcal{P}(\boldsymbol{C}, \boldsymbol{A})$ is expressed as the $\hat{\mathcal{F}}_1$ of Eq. (15), with $\mathbb{Q}_p(\boldsymbol{C}) = q_p(\boldsymbol{C}) \boldsymbol{C}^{\otimes p}$, and $q_p(\boldsymbol{C})$ scalar functions of $\boldsymbol{C}$, so that $\mathcal{P}(\boldsymbol{C}, \boldsymbol{A})$ can be written as a polynomial in I_4:

$$\mathcal{P}(\boldsymbol{C}, \boldsymbol{A}) = \check{\mathcal{P}}(I_4) = q_0(\boldsymbol{C}) + \sum_{p=1}^{N} q_p(\boldsymbol{C}) I_4^p. \tag{43}$$

With these assumptions, $\mathfrak{f}(\mathcal{P}(\boldsymbol{C}, \boldsymbol{A}))$ can be reformulated as a polynomial of degree MN in I_4, i.e.

$$\hat{\mathcal{F}}_1(\boldsymbol{C}, \boldsymbol{A}) = \mathfrak{f}(\mathcal{P}(\boldsymbol{C}, \boldsymbol{A})) = \mathfrak{f}(\check{\mathcal{P}}(I_4)) = a_0(\boldsymbol{C}) + \sum_{h=1}^{MN} a_h(\boldsymbol{C}) I_4^h = a_0(\boldsymbol{C}) + \sum_{h=1}^{MN} a_h(\boldsymbol{C}) \langle \boldsymbol{C} | \boldsymbol{A} \rangle^h, \qquad (44)$$

where each function a_h, with $h \in \{0, \ldots, MN\}$, is obtained by combining the functions q_p of (17) with the coefficients of the polynomial expressing $\mathfrak{f}$. By using the identity (16), which leads to

$$\int\limits_{\mathbb{S}^2 \mathcal{B}} \Psi(\boldsymbol{M}) \langle \boldsymbol{C} | \boldsymbol{A} \rangle^h = \left\langle \boldsymbol{C}^{\otimes h} \middle| \int\limits_{\mathbb{S}^2 \mathcal{B}} \Psi(\boldsymbol{M}) \boldsymbol{A}^{\otimes h} \right\rangle = \langle \boldsymbol{C}^{\otimes h} | \mathbb{H}_h \rangle, \qquad (45)$$

the fibre ensemble can be expressed exactly in terms of the averaged generalised structure tensors $\mathbb{H}_h$, i.e.

$$\mathcal{F}_e = \int\limits_{\mathbb{S}^2 \mathcal{B}} \Psi(\boldsymbol{M}) \hat{\mathcal{F}}_1(\boldsymbol{C}, \boldsymbol{A}) = a_0(\boldsymbol{C}) + \sum_{h=1}^{MN} a_h(\boldsymbol{C}) \langle \boldsymbol{C}^{\otimes h} | \mathbb{H}_h \rangle. \qquad (46)$$

In general, however, for arbitrary functions $\mathfrak{f}$, the approximation (42) is exact in the limit $\boldsymbol{C} \to \boldsymbol{G}$. Indeed, at $\boldsymbol{C} = \boldsymbol{G}$, one obtains $I_4 = I_{40} = \langle \boldsymbol{G} | \boldsymbol{A} \rangle = 1$ and the polynomial

$$\mathcal{P}(\boldsymbol{G}, \boldsymbol{A}) = \check{\mathcal{P}}(1) = q_0(\boldsymbol{G}) + \sum_{p=1}^{N} q_p(\boldsymbol{G}) \qquad (47)$$

becomes constant with respect to the structure tensor, thereby rendering the approximation (42) an identity. Nevertheless, the reliability of (42) deteriorates when $\boldsymbol{C}$ deviates from $\boldsymbol{G}$.

To highlight the loss of accuracy of (42) when $\boldsymbol{C} \neq \boldsymbol{G}$, let us consider a physically relevant example. We set $N = 2$, $q_0(\boldsymbol{C}) = 1$, $q_1(\boldsymbol{C}) = -2$, and $q_2(\boldsymbol{C}) = 1$, so that $\mathcal{P}(\boldsymbol{C}, \boldsymbol{A})$ takes the form

$$\mathcal{P}(\boldsymbol{C}, \boldsymbol{A}) = 1 - 2\langle \boldsymbol{C} | \boldsymbol{A} \rangle + \langle \boldsymbol{C}^{\otimes 2} | \boldsymbol{A}^{\otimes 2} \rangle = (\langle \boldsymbol{C} | \boldsymbol{A} \rangle - 1)^2, \qquad (48)$$

and we assume that the fibre function $\mathcal{F}_1$ represents the anisotropic elastic potential of the Holzapfel–Gasser–Ogden [5] type

$$\hat{\mathcal{F}}_1(\boldsymbol{C}, \boldsymbol{A}) = \hat{W}_{1a}(\boldsymbol{C}, \boldsymbol{A}) = \tfrac{1}{2} c_{1a} \left[\exp\left((\langle \boldsymbol{C} | \boldsymbol{A} \rangle - 1)^2 \right) - 1 \right]. \qquad (49)$$

In this case, after introducing the auxiliary variable $\eta = (\langle \boldsymbol{C} | \boldsymbol{A} \rangle - 1)^2$, the function $\mathfrak{f}$ is identified with

$$\mathfrak{f}(\eta) = \tfrac{1}{2} c_{1a} [\exp(\eta) - 1]. \qquad (50)$$

Since $\mathfrak{f}$ can be expanded in Taylor series about $\eta = 0$, we obtain

$$\mathfrak{f}(\eta) = \tfrac{1}{2} c_{1a} \sum_{n=1}^{+\infty} \frac{\eta^n}{n!}. \qquad (51)$$

Thus, substituting (51) into (42) yields (for brevity, we omit the dependence of functions on their own arguments)

$$\mathcal{F}_e = \int\limits_{\mathbb{S}^2 \mathcal{B}} \Psi \mathfrak{f} = \tfrac{1}{2} c_{1a} \int\limits_{\mathbb{S}^2 \mathcal{B}} \Psi \sum_{n=1}^{+\infty} \frac{\eta^n}{n!} = \tfrac{1}{2} c_{1a} \sum_{n=1}^{+\infty} \frac{1}{n!} \int\limits_{\mathbb{S}^2 \mathcal{B}} \Psi \eta^n. \qquad (52)$$

At each order $n \geq 1$, we write the integral $\int\limits_{\mathbb{S}^2 \mathcal{B}} \Psi \eta^n$ as

$$\int\limits_{\mathbb{S}^2 \mathcal{B}} \Psi \, \eta^n = \left(\int\limits_{\mathbb{S}^2 \mathcal{B}} \Psi \eta \right)^n + \mathfrak{R}_n, \qquad (53)$$

where we refer to $\mathfrak{R}_n$ as to the n-th-order residuum of the approximation. Consequently, (52) can be rewritten as

$$\mathcal{F}_e = \tfrac{1}{2}c_{1a} \sum_{n=1}^{+\infty} \frac{1}{n!} \left(\int_{\mathbb{S}^2\mathcal{B}} \Psi\,\eta \right)^n + \tfrac{1}{2}c_{1a} \sum_{n=1}^{+\infty} \frac{1}{n!}\mathfrak{R}_n. \tag{54}$$

Since the first term on right-hand side of (54) is the exponential of the mean value of η, we obtain

$$\begin{aligned}
\mathcal{F}_e &= \tfrac{1}{2}c_{1a} \sum_{n=1}^{+\infty} \frac{1}{n!} \left(\int_{\mathbb{S}^2\mathcal{B}} \Psi\,\eta \right)^n + \tfrac{1}{2}c_{1a} \sum_{n=1}^{+\infty} \frac{1}{n!}\mathfrak{R}_n \\
&= \tfrac{1}{2}c_{1a} \left[\exp\left(\int_{\mathbb{S}^2\mathcal{B}} \Psi\,\eta \right) - 1 \right] + \tfrac{1}{2}c_{1a} \sum_{n=1}^{+\infty} \frac{1}{n!}\mathfrak{R}_n
\end{aligned} \tag{55}$$

We remark that the residuum $\mathfrak{R}_n$ can be computed exactly at any order. Indeed, it holds true that

$$\begin{aligned}
\mathfrak{R}_n &= \int_{\mathbb{S}^2\mathcal{B}} \Psi\,\eta^n - \left(\int_{\mathbb{S}^2\mathcal{B}} \Psi\,\eta \right)^n \\
&= \sum_{j=0}^{2n} \binom{2n}{j} (-1)^j \langle \boldsymbol{C}^{\otimes(2n-j)} | \mathbb{H}_{2n-j} \rangle - \left(\langle \boldsymbol{C}^{\otimes 2} | \mathbb{H}_2 \rangle - 2\langle \boldsymbol{C} | \boldsymbol{H} \rangle + 1 \right)^n.
\end{aligned} \tag{56}$$

It can be shown, however, that even in the case of an equi-biaxial test (performed on an incompressible material characterised by diagonal matrix representation of $\boldsymbol{C}$, $[\boldsymbol{C}] = \mathrm{diag}\{\lambda^2, \lambda^2, \lambda^{-4}\}$), the residuals may not tend to zero sufficiently fast, even for values of λ sufficiently close to unity. This behaviour contributes to corrupt the reliability of the PARG method and to deteriorate its agreement with the FESD method.

We note that, as it happens for the whole $\hat{\mathcal{F}}_1$ in the general case of Eq. (8), if $\mathcal{P}$ in Eq. (42) is an affine function, i.e. a polynomial of degree one, the PARG method reduces to the GOH method proposed in [6]. The main difference between the PARG method and the GOH method is the level at which the fibre ensemble is approximated. While in the GOH method the averaging integral is performed on the innermost argument, the structure tensor $\boldsymbol{A}$, in the PARG method of Eq. (42), we take the average of the outermost argument, $\mathcal{P}(\boldsymbol{C}, \boldsymbol{A})$, that can be written as a tensor-power polynomial in $\boldsymbol{A}$. We remark that, while the GOH method is applicable to any constitutive function, the PARG method is only applicable when the constitutive function is expressible as a function of a tensor-power polynomial in $\boldsymbol{A}$.

4. Application to elasticity

As an example of application of the integration methods presented in Sect. 3, we look at the averaged physical quantities that are most often sought for in the mechanics of fibre-reinforced materials and biomechanics of soft tissue: elastic potential and stress. Therefore, our physical quantity $\mathcal{F}$ takes the meaning of elastic potential W in Eq. (7), and we write

$$W = \hat{W}(\boldsymbol{C}, \Psi) = \Phi_0\,\hat{W}_0(\boldsymbol{C}) + \Phi_1 \int_{\mathbb{S}^2\mathcal{B}} \Psi(\boldsymbol{M})\,\hat{W}_1(\boldsymbol{C}, \boldsymbol{A}). \tag{57}$$

The averaging integral of the fibre potential W_1 is called the *fibre ensemble potential* [17]:

$$W_e = \hat{W}_e(\boldsymbol{C}, \Psi) = \int_{\mathbb{S}^2\mathcal{B}} \Psi(\boldsymbol{M})\,\hat{W}_1(\boldsymbol{C}, \boldsymbol{A}). \tag{58}$$

In general, it is possible to attribute some "bulk" isotropic stiffness to the fibres, e.g. by using a fibre potential $\hat{W}_1$ given by the sum of an isotropic term and a term depending solely on the anisotropic invariants I_4 and I_5 [18]. The fibre potential $\hat{W}_1$ could therefore be written, as a function $\check{W}_1$ of the invariants, as

$$\check{W}_1(I_1, I_2, I_3, I_4, I_5) = \check{W}_{1i}(I_1, I_2, I_3) + \check{W}_{1a}(I_4, I_5). \tag{59}$$

Furthermore, in those cases in which the contribution of a fibre in direction $\boldsymbol{M}$ is to be ruled out if the direction undergoes contraction, i.e. if $I_4 = \boldsymbol{C} : \boldsymbol{A} < 1$, it is possible to use the Heaviside step function $\mathcal{H}$ evaluated at $I_4 - 1$ and write

$$\check{W}_{1a}(I_4, I_5) = \mathcal{H}(I_4 - 1) \, \check{W}_{1b}(I_4, I_5), \tag{60}$$

where $\check{W}_{1b}$ describes the anisotropic behaviour in extension and is called "base" potential. We remark that, in order to be able to employ the integration methods presented in Sect. 3, we must renounce discriminating between fibres in extension (which are unaffected by the Heaviside step function) and fibres in contraction (which are "killed" by the Heaviside step to reflect the fact that they do not bear load). Indeed, if we were to use the Heaviside step in the fibre potential as in Eq. (59), all approximating potentials presented in Sect. 3 would have to be multiplied by the Heaviside step as well. The Heaviside step with argument $I_4 - 1 = \boldsymbol{C} : \boldsymbol{A} - 1$ would rule out the possibility of a single, direct integration. There are two reasons for this: *a*) it would be in general impossible to know which fibres undergo contraction *a priori*, and one would have to evaluate this at each increment of deformation; *b*) the hypotheses of continuity and differentiability necessary for expandability of functions in Taylor series would be, in general, violated. Therefore, an integration at each increment of deformation would remain the only available solution method, thus defeating the purpose of the proposed approximation methods.

This means that, in terms of range of applicability to the evaluation of the overall elastic behaviour, the methods presented in Sect. 3 are limited to those cases in which all fibres, or at least most of the fibres, are in extension. This can be safely said for tissues with fibres lying mostly on a plane and subjected to tensile plane stress. A typical example is that of blood vessels, which work as inflated-extended tubes under physiological conditions. Schematically, blood vessels can be represented as having, at every point, two dominant fibre directions (with some dispersion) mostly contained in the tangent plane at that point (see, e.g. Figure 1 in [5]).

Remark. We are aware of the existence of mathematical models in which the collagen fibres contribute to the tissue's overall compressive stiffness. It has been recently reported [40] that this is the case, for example, in aged or diseased intervertebral discs, and it was assumed that the fibres' contribution to compressive loads increases with increasing strain magnitude and is influenced by the orientation of the fibres. Still, to the best of our knowledge and understanding, in articular cartilage (the tissue which motivated our current study) no correlation of compressive stiffness with collagen content has been observed [41]. For this reason, we decided to exclude all fibres that are not stretched. Even though this modelling assumption may turn out to be far from reality in some circumstances, we do not make it with the purpose of simplifying the calculations. On the contrary, the necessary introduction of the Heaviside step in the evaluation of the fibre ensemble makes it highly nonlinear in a non-differentiable way, thereby excluding *a priori* the possibility of applying the methods proposed in this work.

For our illustrative purposes, let us choose simple forms of the matrix potential $\hat{W}_0$, isotropic fibre potential $\hat{W}_{1i}$ and (base) anisotropic fibre potential $\hat{W}_{1b}$ (such that $\hat{W}_{1a} = \mathcal{H}(I_4 - 1) \, \hat{W}_{1b}$),

$$\hat{W}_0(\boldsymbol{C}) = \tfrac{1}{2} c_0 \, (I_1(\boldsymbol{C}) - 3), \tag{61a}$$

$$\hat{W}_{1i}(\boldsymbol{C}) = \tfrac{1}{2} c_{1i} \, (I_1(\boldsymbol{C}) - 3), \tag{61b}$$

$$\hat{W}_{1b}(\boldsymbol{C}, \boldsymbol{A}) = \tfrac{1}{2} c_{1a} \left[\exp\left((\boldsymbol{C} : \boldsymbol{A} - 1)^2 \right) - 1 \right], \tag{61c}$$

in which c_0, c_{1i} and c_{1a} are material parameters, and we assume referential volumetric fractions $\Phi_0 = \Phi_1 = 0.5$. The exponential form of the base anisotropic potential in Eq. (61c) has been chosen because it predicts well the characteristic stress response of soft tissues with collagen fibres being undulated in the undeformed configuration, with a toe region and a region of increased stiffness [42]. Moreover, since it consists of the exponential of a polynomial in $I_4 = \boldsymbol{C} : \boldsymbol{A}$, it also allows the use of the PARG method proposed in Sect. 3.3. Note that, although the invariant I_5 should also be included in order to obtain a complete transversely isotropic representation (and avoid unphysical results, see, e.g. [43]), very often I_5 is left out, in order to limit the number of material parameters, and therefore of experimental tests, needed to characterise the material. In passing, we note that the form chosen for $\hat{W}_1$ makes it a particular case of exponential Fung potential [44–47], which is the exponential of a quadratic form in the Green–Lagrange strain. Indeed, by using the definition of Green–Lagrange strain $\boldsymbol{E} = \frac{1}{2}(\boldsymbol{C} - \boldsymbol{G})$, we can write the argument of the exponential in (61c) as a quadratic form in $\boldsymbol{E}$:

$$(\boldsymbol{C} : \boldsymbol{A} - 1)^2 = (\boldsymbol{C} : \boldsymbol{A} - \boldsymbol{G} : \boldsymbol{A})^2 = (2\,\boldsymbol{E} : \boldsymbol{A})^2 = 4\,[\boldsymbol{E} : (\boldsymbol{A} \otimes \boldsymbol{A}) : \boldsymbol{E}]. \tag{62}$$

In a Cartesian (material) reference frame with axes $\boldsymbol{E}_1$, $\boldsymbol{E}_2$, $\boldsymbol{E}_3$, we consider a sample of incompressible soft tissue, which undergoes a biaxial tension test in directions $\boldsymbol{E}_1$ and $\boldsymbol{E}_2$, with a prescribed ratio of the nominal strain in direction 2 to the nominal strain in direction 1, i.e.

$$\zeta = \frac{\lambda_2 - 1}{\lambda_1 - 1}. \tag{63}$$

In an isochoric ($J = \det \boldsymbol{F} = 1$) biaxial test in directions $\boldsymbol{E}_1$ and $\boldsymbol{E}_2$, with nominal strain ratio ζ, the matrix representations of the deformation gradient $\boldsymbol{F}$ and the right Cauchy-Green deformation $\boldsymbol{C}$ are

$$[\boldsymbol{F}] = \mathrm{diag}\left[\lambda,\ \zeta(\lambda - 1) + 1,\ \frac{1}{\lambda(\zeta(\lambda - 1) + 1)}\right], \tag{64}$$

$$[\boldsymbol{C}] = \mathrm{diag}\left[\lambda^2,\ (\zeta(\lambda - 1) + 1)^2,\ \frac{1}{\lambda^2(\zeta(\lambda - 1) + 1)^2}\right], \tag{65}$$

so that $\zeta = 1$ describes an equi-biaxial test, for which $[\boldsymbol{F}] = \mathrm{diag}[\lambda, \lambda, \lambda^{-2}]$ and $[\boldsymbol{C}] = \mathrm{diag}[\lambda^2, \lambda^2, \lambda^{-4}]$, $0 < \zeta < 1$ means that direction $\boldsymbol{E}_1$ is being stretched more than direction $\boldsymbol{E}_2$, and $\zeta > 1$ vice versa.

We assume that the fibres are oriented according to a transversely isotropic von Mises distribution (see, e.g. [6,20,48]),

$$\varrho(\Theta) = \frac{1}{\pi}\sqrt{\frac{b}{2\pi}}\frac{\exp[b(\cos(2\Theta) + 1)]}{\mathrm{erfi}(\sqrt{2b})}, \tag{66}$$

where Θ is the angle between the generic direction $\boldsymbol{M}$ and the axis of transverse isotropy $\boldsymbol{M}_0$, $\mathrm{erf}(x)$ and $\mathrm{erfi}(x) = -i\,\mathrm{erf}(i\,x)$ denote the error function at x and the imaginary error function at x, respectively [49], and b is called concentration parameter. In the form reported in Eq. (66), the von Mises distribution can accommodate both positive and negative values of the concentration parameter [19,48,50]. The limit $b \to +\infty$ describes fibres all aligned in the direction $\boldsymbol{M}_0$ of the axis of symmetry, the limit $b \to 0$ represents isotropy, and the limit $b \to -\infty$ describes fibres all lying on the transverse plane, which is, by definition, orthogonal to the direction of the axis of symmetry $\boldsymbol{M}_0$. For simplicity, we assume that the axis of symmetry $\boldsymbol{M}_0$ coincides with the direction $\boldsymbol{E}_1$ of axis 1 of the biaxial test (Fig. 1).

The approximated integration methods proposed in Sect. 3 are applied to the calculation of the ensemble potential $\hat{W}_e$ with the provision that, even if the fibres are modelled as extension-only, i.e. $\hat{W}_{1a} = \mathcal{H}(I_4 - 1)\hat{W}_{1b}$, the approximation is made with $\hat{W}_{1a} \equiv \hat{W}_{1b}$. Indeed, as noted above, we *must* renounce to excluding the fibres in contraction when employing our approximation methods. The three proposed methods are implemented with the assumptions outlined below:

1. INEX: the expansion is performed about $\bar{I}_{40} = 1$ as outlined in Sect. 3.1 and is truncated at order 6, which, in contrast with what happens with the structure tensor expansion STEX, is still computationally manageable;

2.   STEX: the expansion is performed about the structure tensor $\boldsymbol{A}_0 = \boldsymbol{M}_0 \otimes \boldsymbol{M}_0$ of the direction $\boldsymbol{M}_0 \equiv \boldsymbol{E}_1$ of the axis of symmetry of the potential; the expansion is truncated at order 4, which is the maximum order of expansion that the computational resources in our hands allowed;

3.   PARG: the outermost argument of polynomial form in the fibre potential $\hat{W}_1$ of Eq. (61c) is given by $(\boldsymbol{C} : \boldsymbol{A} - 1)^2$, the directional average of which is evaluated.

The three proposed methods are compared against:

4.   GOH: replacement of the structure tensor $\boldsymbol{A}$ in Eq. (61c) with the directional average $\boldsymbol{H}$ of Eq. (18) [6];

5.   FESD: integration of the fibre ensemble, at each increment of deformation, by means of the method of the spherical t-designs; note that all fibres, in extension and contraction, are taken into account, i.e. as in the three proposed methods, we consider $\hat{W}_{1a} \equiv \hat{W}_{1b}$;

6.   FESDH: integration of the fibre ensemble at the each increment of deformation, as originally introduced in [20] for the elastic properties, i.e. with the fibre potential $\hat{W}_{1a} = \mathcal{H}(I_4 - 1) \hat{W}_{1b}$, that "kills" the fibres in contraction; this is done to verify under which conditions "sparing" the fibres in contraction is an acceptable approximation.

The method for the evaluation of the stresses is provided in Appendix E. The values of the elastic potential W and the total Cauchy stresses σ^{11} and σ^{22} are plotted as a function of the stretch λ under the deformation described by Eq. (65) and are normalised with respect to the material parameter c_0 of Eq. (61a), while c_{1i} and c_{1a} are assumed to have the values $0.5\,c_0$ and $5\,c_0$, respectively. At a given value of the strain ratio ζ, a set of three plots (W, σ^{11} and σ^{22}) is produced for each value of the concentration
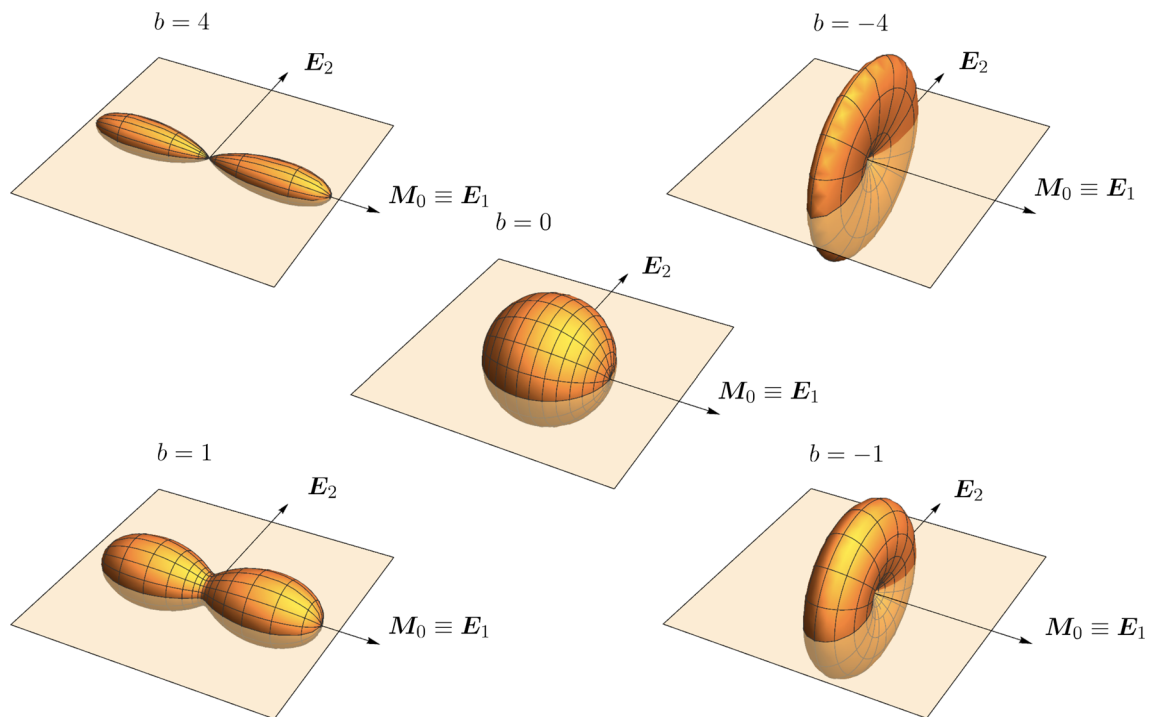

FIG. 1. Fibre arrangement for the samples undergoing biaxial test in the plane of directions $\boldsymbol{E}_1$ and $\boldsymbol{E}_2$. The orientation of the fibres follows a von Mises distribution with axis of symmetry $\boldsymbol{M}_0$ parallel to $\boldsymbol{E}_1$. The cases of $b = 4$ (fibres mostly aligned in the direction of symmetry), $b = 1$, $b = 0$ (fibres isotropically distributed), $b = -1$ and $b = -4$ (fibres mostly lying on the transverse plane) are shown as an example

parameter b equal to 4 (strong alignment in the direction of symmetry of the probability distribution), 1 (weak alignment), 0 (isotropic distribution), -1 (weak alignment on the transverse plane), -4 (strong alignment). Figure 2 reports the plots obtained for $\zeta = 1$ (equi-biaxial test), Fig. 3 for $\zeta = 0.5$ (direction $\boldsymbol{E}_1$ stretched more than direction $\boldsymbol{E}_2$) and Fig. 4 for $\zeta = 2$ (direction $\boldsymbol{E}_2$ stretched more than direction $\boldsymbol{E}_1$). All calculations were performed with *Mathematica* (Wolfram Research, Champaign, Illinois, USA).

We note (Fig. 1) that the fibre distribution with negative values of the concentration parameter b is quite unrealistic: in a quasi-two-dimensional sample of a real soft tissue, very few fibres would be oriented out-of-plane. We chose to keep this distribution, particularly for the quite extreme case of $b = -4$, because most of the fibres are oriented out-of-plane, and therefore undergo contraction. This offers a way to verify what discrepancy the fibres in contraction cause between the results of the FESD calculation that does not exclude them and those of the FESDH calculation that does exclude them.

5. Results

The FESDH method, including the Heaviside function in order to "kill" the fibres in contraction, is regarded as the "correct" computation, in so far as it rigorously follows the rule of mixtures as in Eqs. (7) and (57). For the tested values of the concentration parameter b and the strain ratio ζ, the FESD that does not discriminate between fibres in extension and contraction gives very close results to the "correct" FESDH method, except for some discrepancy, mainly in the potential, for the case of large negative b. A discrepancy between FESD and FESDH is expected as, for large negative b, the orientation of a quite large fraction of the fibres is close to the $\boldsymbol{E}_3$ (out-of-plane) direction, and these fibres are therefore in contraction. However, the discrepancy is much smaller than expected (see e.g. the plots for $b = -1$ and $b = -4$ in Fig. 3).

Among all tested methods, the INEX method is systematically the one that gives the results closest to those of FESDH/FESD for all values of b in the equi-biaxial case (Fig. 2), almost always in the case of $\zeta = 0.5$, except in a few cases in which it is slightly outperformed by the PARG method and the GOH method (e.g. potential and stresses for $b = 4$, Fig. 3). For $\zeta = 2$, while the INEX method is generally the second closest to the spherical designs method (after the STEX method, as mentioned below), the fit is not as good as in the cases of $\zeta = 1$ and $\zeta = 0.5$.

The STEX method is by far the most inappropriate. As expected, it works best when the probability Ψ is peaked around the direction $\boldsymbol{M}_0$ about which the expansion is performed. For the considered von Mises probability, this situation corresponds to values of the concentration parameter b greater than zero. Indeed, for the fairly large value $b = 4$, it is very close to the FESDH/FESD method. However, even for $b = 4$, it fails to describe a physically correct behaviour for the stress in direction 2, when $\zeta = 0.5$ (Fig. 3). The results become generally disastrous for lower values of b, with several occurrences of unphysical behaviour (i.e. decreasing stress in direction 2 for increasing strain), although in some cases (e.g. particularly for $\zeta = 2$, Fig. 4) the STEX method evaluates the potential very accurately, even for small or negative b.

The PARG method turned out to be a fairly reasonable approximation of the FESDH/FESD method. For the equi-biaxial test (Fig. 2) and for $\zeta = 2$ (Fig. 4), it is more accurate for positive values of b. However, this trend is reversed for $\zeta = 0.5$ (Fig. 3), i.e. the PARG works better for negative values of b. In general, for given b and ζ, the values of the potential and the stresses yielded by the PARG method lie between those of the INEX and the GOH methods, with a few exceptions (e.g. $b = 4$ in the equi-biaxial test and $b = 4, -4$ for $\zeta = 0.5$) where the PARG method is the closest to the FESDH/FESD method. For all tested conditions, the PARG method is closer to the FESDH/FESD method than the GOH method is.

The GOH method has a good agreement with the FESDH/FESD method for large positive values of the concentration parameter b. However, for $b = 0$ (isotropic distribution) and negative values of b, the
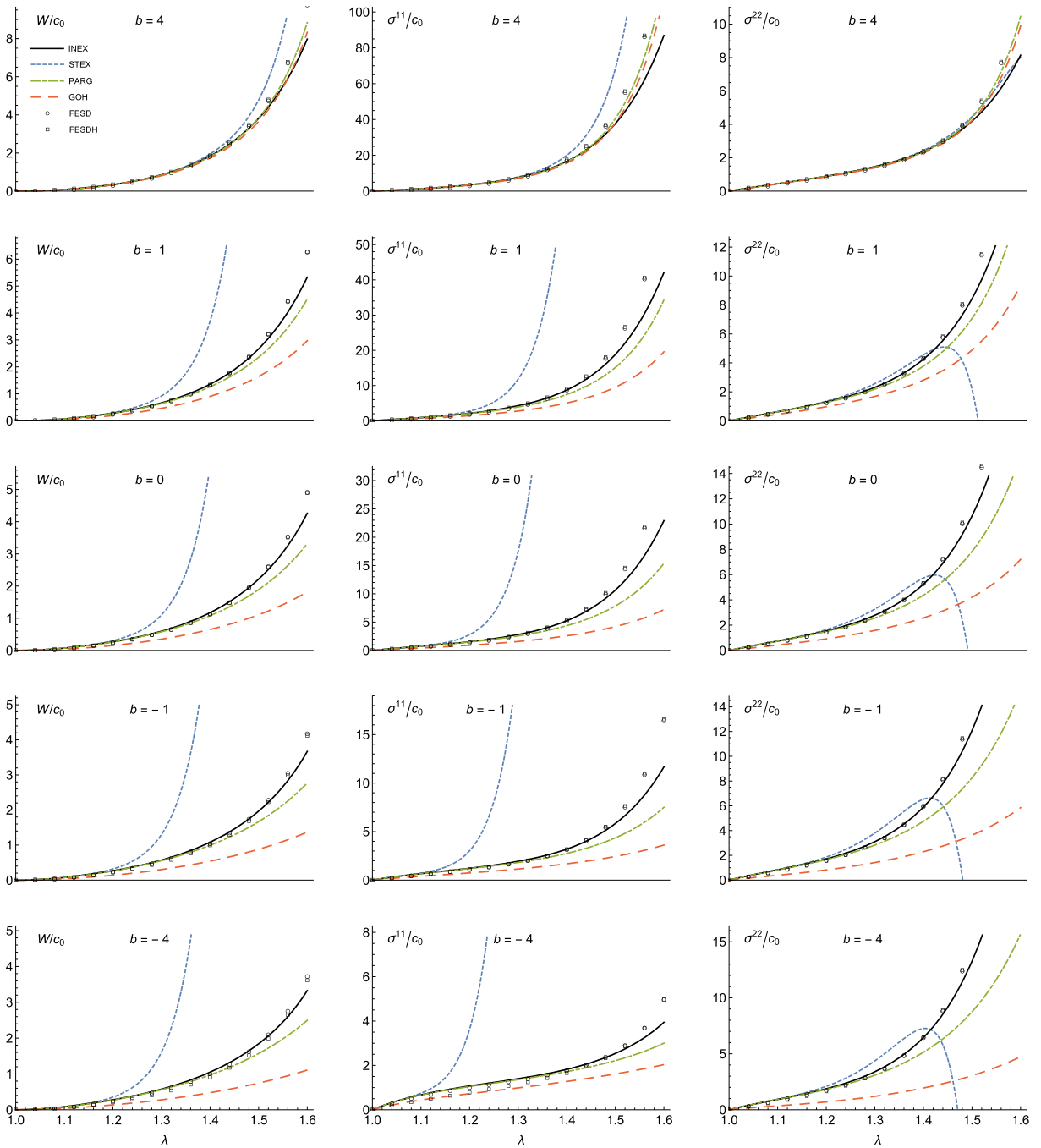
FIG. 2. Elastic potential and stress for the equi-biaxial test ($\zeta = 1$)

behaviour of the GOH method deviates quite substantially from that of the FESDH/FESD method. For the tested values of b and ζ, the behaviour of the GOH method is easily predictable, in the sense that, for a given ζ, a higher value of b necessarily means a behaviour closer to FESDH/FESD, and there seems to be no exceptions.
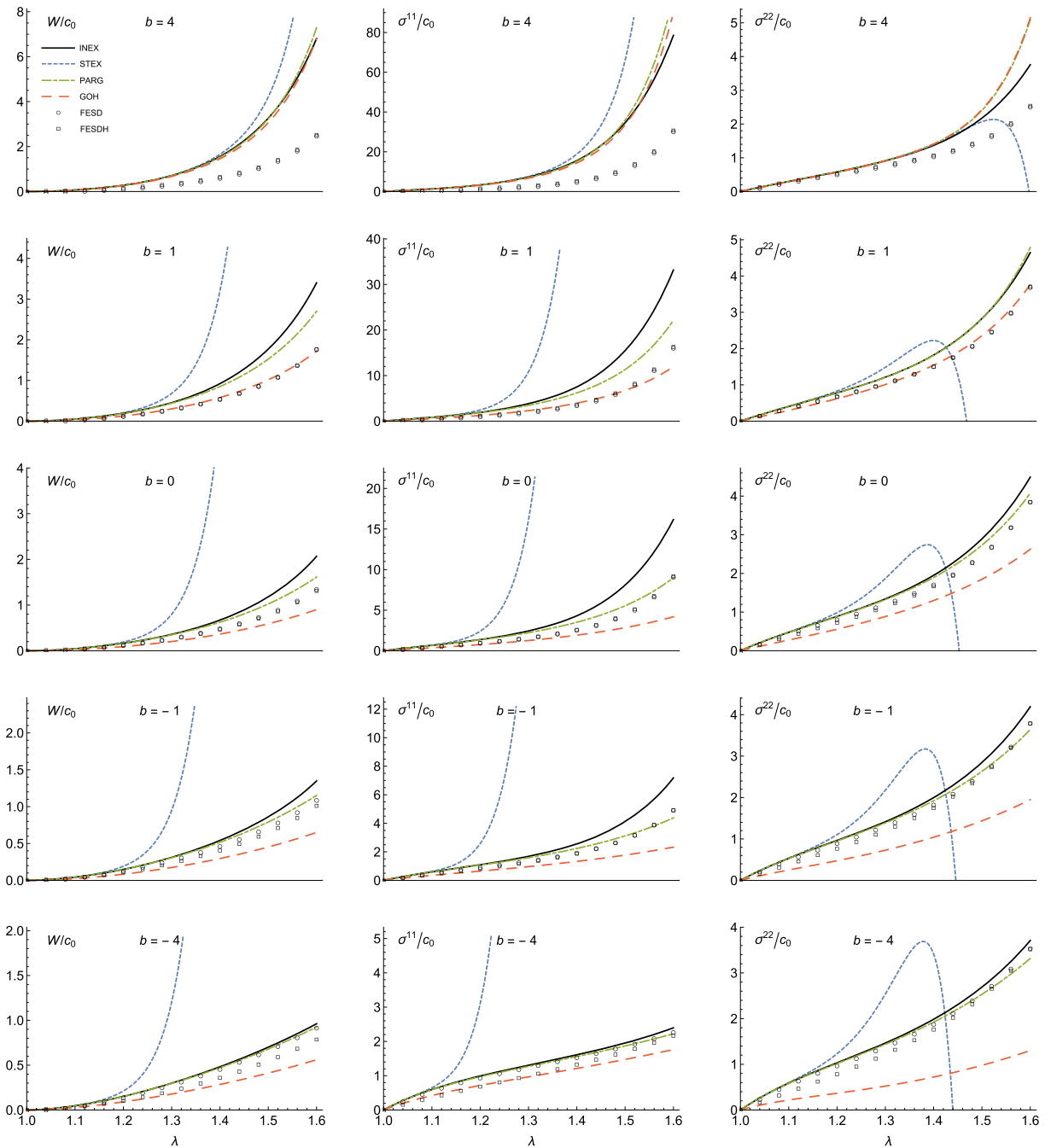
Fɪɢ. 3. Elastic potential and stress for a biaxial test with $\zeta = 0.5$

To give an idea about the computational time for each method, we show in Table 1 the time required to produce the curves for the equi-biaxial test reported in Fig. 2 for $b = 4$. In order to examine quantitatively the accuracy of the proposed methods, we provide in Figs. 5a, b the curves describing, for two different values of the concentration parameter b, the absolute error of the elastic potential W, computed for
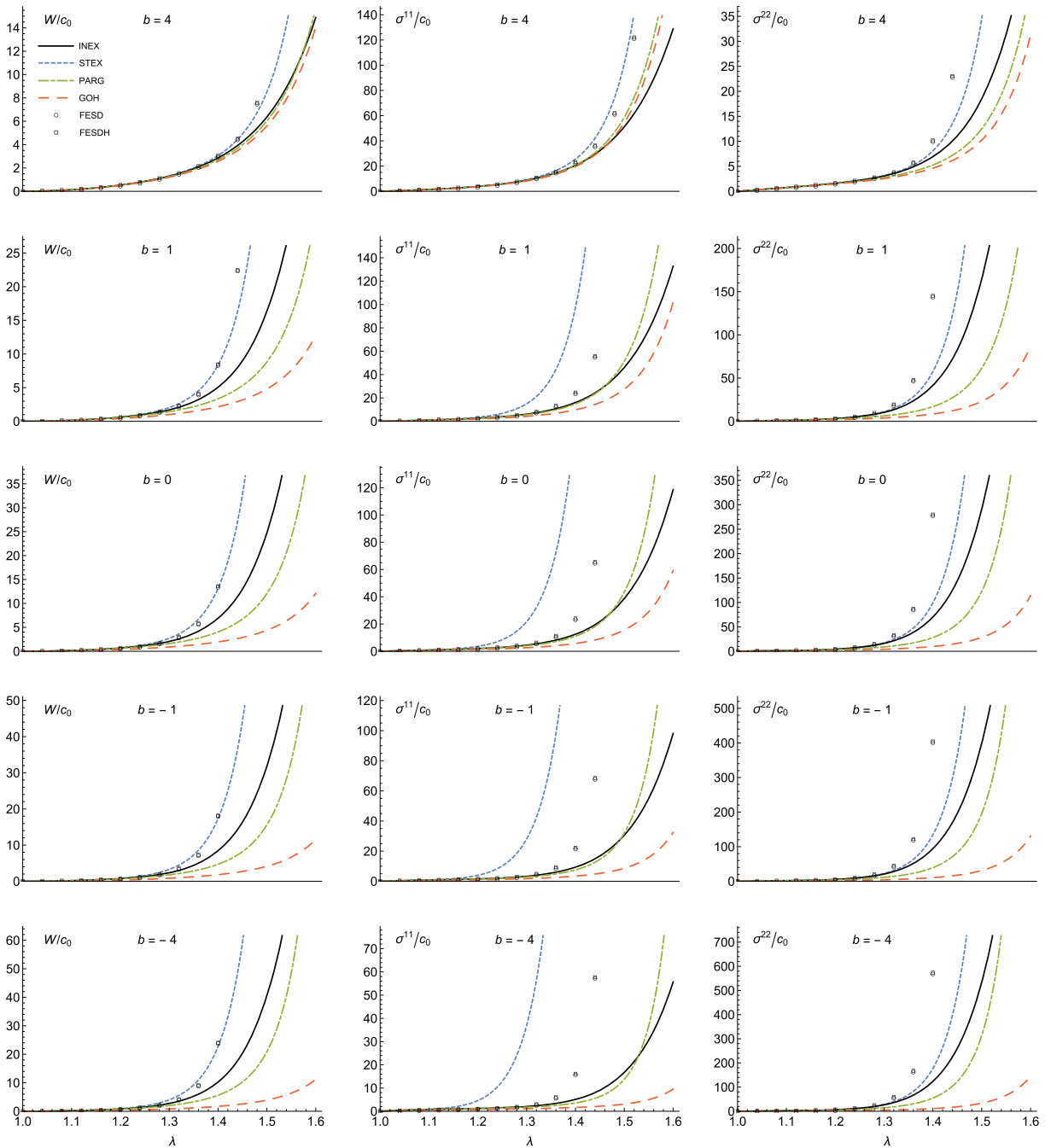
FIG. 4. Elastic potential and stress for a biaxial test with $\zeta = 2$

$\lambda \in [1.0, 1.6]$ by regarding the FESDH method as the reference one, i.e. $\mathcal{E}_{\mathrm{M}} := |W_{\mathrm{M}} - W_{\mathrm{FESDH}}|$, with $\mathrm{M} \in \{\mathrm{STEX}, \mathrm{INEX}, \mathrm{PARG}, \mathrm{GOH}, \mathrm{FESD}\}$. The thin, black lines corresponding to the values of the absolute error 0.05 for $b = 4$, and 0.1 for $b = -4$ define a threshold that identifies, for each value of the concentration parameter, a maximal range of validity, i.e. the maximal subset of the stretch interval $[1.0, 1.6]$ within

TABLE 1. *Computational time (s) for graphs at $\zeta = 1$ and $b = 4$ and stretch range $\lambda \in [1.0, 1.6]$; time increment in FESD and FESDH is $40\,ms$*

Quantity	STEX	INEX	PARG	GOH	FESD	FESDH
Elastic potential W	0.66	0.06	0.05	0.06	1.66	2.81
Stress σ^{11}	0.78	0.44	0.08	0.14	25.20	38.80
Stress σ^{22}	0.19	0.55	0.08	0.06	25.34	38.17
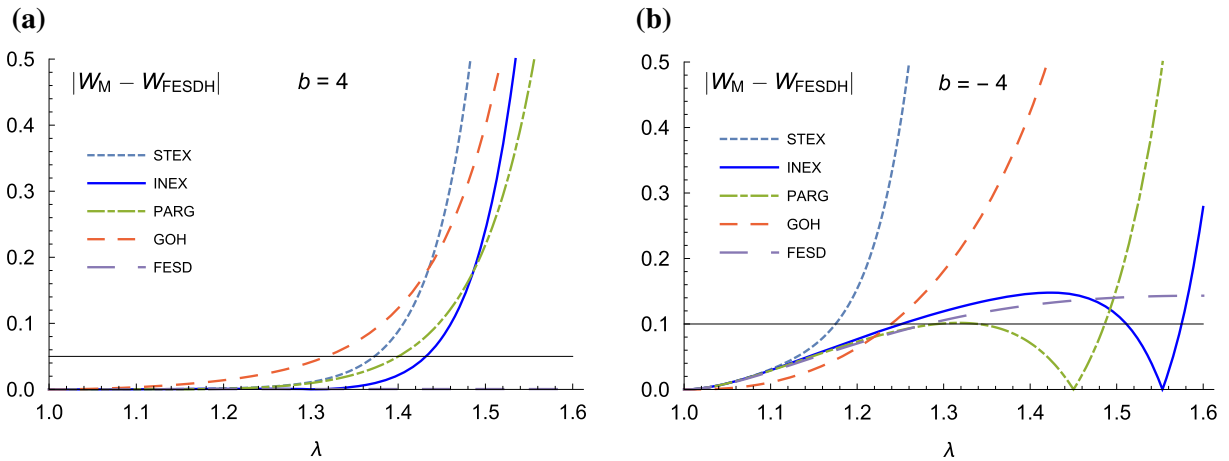
FIG. 5. Absolute error $|W_{\mathrm{M}} - W_{\mathrm{FESDH}}|$ of the elastic potential W, with $\mathrm{M} \in \{\mathrm{STEX}, \mathrm{INEX}, \mathrm{PARG}, \mathrm{GOH}, \mathrm{FESD}\}$, for two different values of the concentration parameter, $b = 4$ and $b = -4$

TABLE 2. *Relative error (%) for the elastic potential W, in the equi-biaxial test ($\zeta = 1$) and at $\lambda = 1.3$*

b	FESD	INEX	STEX	PARG	GOH
4	0.06	0.04	1.30	1.13	4.85
1	3.87	4.63	45.35	1.26	26.92
0	9.20	10.26	102.85	6.44	14.86
-1	14.99	16.45	163.98	12.49	29.02
-4	23.02	25.99	250.77	21.95	39.35

TABLE 3. *Relative error (%) for the stress σ^{11}, in the equi-biaxial test ($\zeta = 1$) and at $\lambda = 1.3$*

b	FESD	INEX	STEX	PARG	GOH
4	0.0007	0.7728	3.5272	2.9521	6.9328
1	0.7915	1.2773	181.0450	6.5662	34.0420
0	3.0387	3.8109	552.9186	4.2988	41.0398
-1	7.6397	8.7854	1205.4554	2.3712	35.4135
-4	20.4896	22.8115	2664.3860	19.3050	13.5467

which the absolute error is assumed to be acceptable. Furthermore, for a given value of λ belonging to this range, i.e. $\lambda = 1.3$, Tables 2 and 3 report the values of the relative error of the elastic potential and the stress σ^{11} for varying concentration parameter b. In doing this, we take the FESDH method as the term of comparison.

Clearly, the results obtained by using the FESD approach are by far the closest to the ones determined by FESDH. This is because the two procedures differ from each other only by the presence of the Heaviside step function. Thus, for situations in which almost all fibres are stretched, there is virtually no difference

between FESD and FESDH. In contrast, when there is a substantial fraction of fibres that are not stretched, the results obtained by employing the FESD deviate from those predicted by the FESDH. Specifically, both the amplitude and the sense of the deviations depend on the stretch λ, concentration parameter b and deformation mode ζ. For example, the FESD overestimates the values of W/c_0 for $\zeta = 1$ and $b = -4$ (cf. Fig. 2), while it underestimates them for $\zeta = 2$ and $b = -4$ (cf. Fig. 4). Looking at Table 2, we also notice that, in contrast to what happens for all other methods, the relative error pertaining to INEX decreases with decreasing b, i.e. when the fibres tend to lie transversely to the symmetry axis. We argue that this result is related to the fact that the INEX method does not select any particular structure tensor for the Taylor expansion formula approximating the elastic potential. On the contrary, since the STEX method necessitates to specify the structure tensor around which the Taylor expansion formula is constructed, it produces a comparatively small absolute error (cf. Fig. 5a) when the fibres are concentrated around a given direction ($b = 4$), while its accuracy deteriorates for decreasing b, i.e. when the fibres tend to deviate from that direction.

We notice that, for $b = 4$, the INEX and PARG approximations are the closest to FESDH/FESD. For the case of PARG, this may be due to the fact that this method does not substitute $\hat{\mathcal{F}}_1$ with its Taylor polynomial but, rather, it calculates an *exact* average of the polynomial argument of the fibre constitutive function. Thus, the more the fibres are peaked around a given direction, the more accurate the PARG method becomes. Looking at the columns of Tables 2 and 3 relative to the INEX and PARG methods, we notice that the choice of the "optimal" approximation criterion is quite problem-dependent (i.e. it depends on b). Consequently, there could be cases (e.g. in inhomogeneous problems, or if b changes in time due to some sort of tissue remodelling) in which the approximation method has to be chosen adaptively, thereby switching from one to the other in order to minimise the error. For completeness, we mention that the relative errors associated with the stress σ^{11} are not monotonic functions of b for the FESD and the PARG methods. A plausible explanation for this behaviour could be their capability of resolving the fibre orientation with increasing dispersion (i.e. with $b \to -\infty$).

All the methods belonging to the class of approximations not calling for step-by-step integrations (such as the algorithms based on the spherical designs) fail to be accurate after some "threshold" value of the stretch that depends on the deformation mode (biaxial, equi-biaxial, etc.) as well as on the concentration parameter associated with the chosen probability density distribution.

As is visible in the plots of the components of Cauchy stress, the main influence on the monotonicity and convexity of the curves is given by the interplay between the concentration parameter, b, which characterises the von Mises distribution, and the parameter ζ, which defines the deformation mode. In particular, for $\zeta = 1$ and $\zeta = 0.5$, the stress curves lose convexity with decreasing b. Indeed, when the deformation along the symmetry axis is greater than, or equal to, the deformation in the transverse plane, on which the fibres tend to lie for decreasing b, the STEX method is the one that deviates the most from the FESDH predictions, thereby introducing unphysical stiffnesses (cf. e.g. Figs. 2 and 3).

Moreover, a computation of the stress, e.g. σ^{11}, shows that the summand of σ^{11} responsible for the concavity in the stress curves is given by the Lagrange multiplier introduced to account for the incompressibility constraint. To show that this is actually the case, we take as example the stress approximated by means of the INEX method. Hereafter, for ease of demonstration, we write its expression only for the Taylor expansion of the elastic potential up to the second order. In the figures, however, we show also the stress for the case of an expansion up to the sixth order. By using the elastic potential (57), along with (61a)–(61c) and arresting the Taylor expansion of $\hat{W}_1(\boldsymbol{C}, \boldsymbol{A})$ at the order $n = 2$, the approximated expression of the constitutive part of the second Piola–Kirchhoff stress tensor reads

$$\boldsymbol{S}_{\text{c}}^{\text{app}} := 2\frac{\partial \hat{W}}{\partial \boldsymbol{C}}(\boldsymbol{C}) = \Phi_0\, c_0\, \boldsymbol{G}^{-1} + \Phi_1\, c_{1i}\, \boldsymbol{G}^{-1} + \boldsymbol{S}_{1a}^{\text{app}}, \tag{67}$$

where [cf. (98)]

$$\boldsymbol{S}_{1a}^{\text{app}} = 2\Phi_1 c_{1a}[\mathbb{H}_2 : \boldsymbol{C} - \mathbb{H}_1]. \tag{68}$$
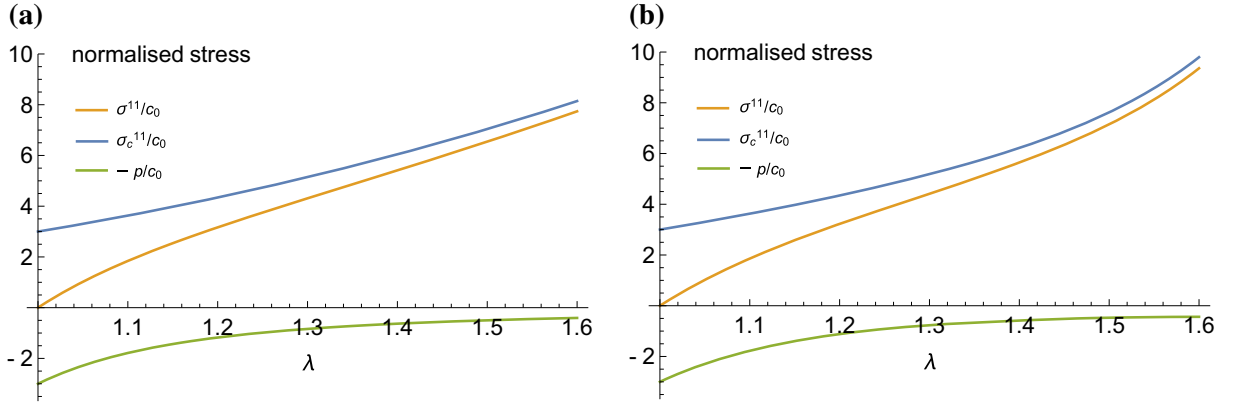
(a)

(b)

FIG. 6. Normalised stresses and pressure for the INEX method: **a** order 2, **b** order 6

Because of the imposed incompressibility, the overall second Piola–Kirchhoff stress tensor is given by $\boldsymbol{S}^{\mathrm{app}} = -p\boldsymbol{C}^{-1} + \boldsymbol{S}_{\mathrm{c}}^{\mathrm{app}}$, where p is the Lagrange multiplier (*not* coinciding with the pressure in the present treatment) associated with the incompressibility constraint. Accordingly, for an equi-biaxial test (i.e. when $[\boldsymbol{C}] = \mathrm{diag}\{\lambda^2, \lambda^2, \lambda^{-4}\}$), the component σ^{11} of the Cauchy stress tensor becomes

$$\sigma^{11} = -p + (\Phi_0 c_0 + \Phi_1 c_{1i})\lambda^4 + \sigma_{1a}^{11}, \tag{69}$$

with $\sigma_{\mathrm{c}}^{11} := (\Phi_0 c_0 + \Phi_1 c_{1i})\lambda^4 + \sigma_{1a}^{11}$ being the constitutive part of σ^{11} and

$$\sigma_{1a}^{11} = 2\Phi_1 c_{1a}\big[(\mathbb{H}_2)^{1111}\lambda^4 + (\mathbb{H}_2)^{1122}\lambda^4 + (\mathbb{H}_2)^{1133}\frac{1}{\lambda^2} - (\mathbb{H}_1)^{11}\lambda^2\big]. \tag{70}$$

Plotting σ^{11} versus λ shows that σ_{c}^{11} is a convex function of λ, whereas the negative of the Lagrange multiplier, $-p$, is a concave function λ. Since σ_{c}^{11} grows almost linearly for values of λ close to unity, the composition $\sigma^{11} = -p + \sigma_{\mathrm{c}}^{11}$ turns out to be non-convex. This is depicted in Fig. 6a, b, where the effect of raising the order of the approximation is testified by the increasing curvature, for large enough values of λ of the constitutive part of stress.

6. Summary and discussion

In a biological tissue (or industrial material) with a statistical distribution of reinforcing fibres, the effect of the fibres on the overall constitutive function $\hat{\mathcal{F}}$ of a given physical quantity can be obtained by integrating the fibre constitutive function $\hat{\mathcal{F}}_1$, weighted by an orientation probability distribution, over the set of all directions in space [cf. Eq. (7)]. The resulting integral, called fibre ensemble $\hat{\mathcal{F}}_e$ in this work [cf. Eq. (8)], can in general only be evaluated numerically at each increment of deformation, since the deformation (usually represented by the right Cauchy-Green deformation tensor $\boldsymbol{C}$) cannot be factorised out of the integral sign, except in the case in which $\hat{\mathcal{F}}_1$ is expressed as a tensor-power polynomial in the structure tensor $\boldsymbol{A}$ [19]. Even though the numerical integration of $\hat{\mathcal{F}}_e$ is flexible and can be made very accurate, it is sometimes computationally expensive. Indeed, especially in time-dependent nonlinear problems, it has to be "called" at each time step and at each iteration of some nonlinear solver, thereby increasing computational costs. With the aim of containing these costs, we exploited polynomials to achieve a single, direct integration of a given fibre constitutive function $\hat{\mathcal{F}}_1$ and thus an approximation of the corresponding fibre ensemble $\hat{\mathcal{F}}_e$. We elaborated three methods: a Taylor expansion in the transversely isotropic invariants (INEX method), which we presented in the case of functions of the fourth invariant

I_4 alone, but which can be seamlessly extended to functions including also the fifth invariant, I_5; a Taylor expansion in the structure tensor $\boldsymbol{A}$ about a given value $\boldsymbol{A}_0$ corresponding to a direction $\boldsymbol{M}_0$ (STEX method); and, for the case of fibre constitutive functions $\hat{\mathcal{F}}_1$ expressed as some function of a polynomial $\mathcal{P}(\boldsymbol{C}, \boldsymbol{A})$, the replacement of $\mathcal{P}(\boldsymbol{C}, \boldsymbol{A})$ with its directional average (PARG method). The latter method is similar to the GOH method proposed in [6]. We emphasise that our methods are not meant to replace the step-by-step integration, which is considered to be the most accurate method to represent a constitutive function expressed by the rule of mixtures, and was regarded as term of comparison to test the accuracy of our approximations. Rather, our methods aim to offer alternative options to step-by-step integration schemes, such as the FESD and the FESDH, since the direct integration of constitutive functions can be performed *before* discretising the system in time and before starting any iterative scheme for solving nonlinear problems.

We chose to test the proposed methods for the case of the elastic potential and the associated stress. We compared the proposed methods to the "exact" integration, performed at each increment of deformation by means of the method of the spherical designs [20,21,34], which we have called here FESD method, as well as to the GOH method [6]. A calculation including the Heaviside function was made with the method of the spherical designs (FESDH method) in order to eliminate the contribution of the fibres in contraction and to estimate in which conditions counting also the fibres undergoing contraction is acceptable.

As mentioned in Sect. 5, for most of the tested conditions, the INEX method (expansion in the invariants) was the closest to the "rigourous" integration performed with FESDH/FESD method (fibre ensemble evaluated by means of the method of the spherical designs, with or without the Heaviside function to eliminate the fibres in contraction). What really distinguishes the INEX method from the other ones is that its accuracy is weakly dependent on the distribution of the fibres (concentration parameter b). Moreover, one could improve the accuracy of the approximation by simply computing a higher-order expansion. In contrast, the accuracy of the other tested methods shows a clear dependence on the distribution of the fibres, i.e. their accuracy is higher for high values of b and decreases, often sensibly, as b becomes negative.

In conclusion, when implementing the fibre ensemble (Eq. (8)) arising from the rule of mixtures into finite elements, the method of Taylor expansion in the invariants (INEX) constitutes a valid, computationally inexpensive, direct integration method, alternative to programming a complex user subroutine that employs the method of the spherical designs to perform the directional averages at each increment of deformation. The integrals $\mathbb{H}_p$ needed in the INEX method (Eqs. (27) and (35)) can be evaluated directly (Eq. (13)) with a commercially available calculation package such as *Mathematica* (Wolfram Research, Champaign, Illinois, USA), and then exported into a much simpler user subroutine to be used in the finite element code. In fact, once the highest order $2n$ of the expansion is set, one can simply calculate the corresponding tensor $\mathbb{H}_n$ and then obtain all tensors $\mathbb{H}_p$ of lower order $2 \le 2p < 2n$ by contracting any $n - p$ pairs of indices [31]. Moreover, for the case of the von Mises distribution, which is determined univocally by the concentration parameter b, the tensors $\mathbb{H}_p$ can be exported as functions of b, which has the obvious advantage of providing a function rather than an array of values. It is in our future plans to develop similar methods for fibre-reinforced biological tissues seen as higher-gradient materials (see, e.g. [51–53]).

Acknowledgments

Appendix A. Continuum mechanics notation and definitions

The deformation χ maps material points $X = (X^1, X^2, X^3)$ in the reference configuration $\mathcal{B}$ into spatial points $x = (x^1, x^2, x^3)$ in the physical space $\mathcal{S}$. The deformation gradient $\boldsymbol{F}$ has components $F^a{}_A = \chi^a{}_{,A}$ and pushes-forward material vectors $\boldsymbol{W}$ with components W^A into spatial vectors $\boldsymbol{FW}$ with components $F^a{}_A W^A$. The inverse $\boldsymbol{F}^{-1}$ pulls-back spatial vectors $\boldsymbol{w}$ with components w^a into material vectors $\boldsymbol{F}^{-1}\boldsymbol{w}$ with components $(\boldsymbol{F}^{-1})^A{}_a w^a$. The transpose $\boldsymbol{F}^{\mathrm{T}}$ pulls-back spatial covectors $\boldsymbol{\pi}$ with components π_a into material covectors $\boldsymbol{F}^{\mathrm{T}}\boldsymbol{\pi}$ with components $(\boldsymbol{F}^{\mathrm{T}})_A{}^a \pi_a = F^a{}_A \pi_a$. The inverse transpose $\boldsymbol{F}^{-T}$ pushes-forward material covectors $\boldsymbol{\Pi}$ with components Π_A into spatial covectors $\boldsymbol{F}^{-T}\boldsymbol{\Pi}$ with components $(\boldsymbol{F}^{-T})_a{}^A \Pi_A = (\boldsymbol{F}^{-1})^A{}_a \Pi_A$. The determinant $J = \det \boldsymbol{F}$ is called volume ratio and measures volumetric deformation.

The reference configuration $\mathcal{B}$ and the physical space $\mathcal{S}$ are equipped with metric tensors $\boldsymbol{G}$ and $\boldsymbol{g}$, respectively, which define the scalar products of material and spatial vectors as $\langle \boldsymbol{W}, \boldsymbol{Y} \rangle = \boldsymbol{W}.\boldsymbol{Y} = \boldsymbol{W}\boldsymbol{G}\boldsymbol{Y} = W^A G_{AB} Y^B$ and $\langle \boldsymbol{w}, \boldsymbol{y} \rangle = \boldsymbol{w}.\boldsymbol{y} = \boldsymbol{w}\boldsymbol{g}\boldsymbol{y} = w^a g_{ab} y^b$, respectively. The pull-back of the spatial metric $\boldsymbol{g}$ is the right Cauchy-Green deformation tensor $\boldsymbol{C} = \boldsymbol{F}^{\mathrm{T}}\boldsymbol{g}\,\boldsymbol{F} = \boldsymbol{F}^{\mathrm{T}}.\boldsymbol{F}$, with components $(\boldsymbol{F}^{\mathrm{T}})_A{}^a g_{ab} F^b{}_B = F^a{}_A g_{ab} F^b{}_B$. The pull-back of the inverse spatial metric $\boldsymbol{g}^{-1}$ is the Piola deformation tensor $\boldsymbol{B} = \boldsymbol{F}^{-1}\boldsymbol{g}^{-1}\boldsymbol{F}^{-T} = \boldsymbol{F}^{-1}.\boldsymbol{F}^{-T} = \boldsymbol{C}^{-1}$, with components $(\boldsymbol{F}^{-1})^A{}_a g^{ab}(\boldsymbol{F}^{-T})_b{}^B = (\boldsymbol{F}^{-1})^A{}_a g^{ab}(\boldsymbol{F}^{-1})^B{}_b$. The difference between the *pulled-back material metric* $\boldsymbol{C}$ and the natural material metric $\boldsymbol{G}$, normalised by the coefficient $1/2$, is the Green–Lagrange strain $\boldsymbol{E} = \frac{1}{2}(\boldsymbol{C} - \boldsymbol{G})$.

Appendix B. Invariants of the deformation

Isotropy is the material symmetry defined as the invariance of a given physical quantity with respect to the whole group of rotations [54]. For an isotropic material, the three scalar invariants of the deformation are

$$I_1 = \mathrm{tr}\,(\boldsymbol{C}) = \boldsymbol{G}^{-1} : \boldsymbol{C}, \tag{71a}$$

$$I_2 = \tfrac{1}{2}\,[(\mathrm{tr}(\boldsymbol{C}))^2 - \mathrm{tr}(\boldsymbol{C}^2)], \tag{71b}$$

$$I_3 = \det(\boldsymbol{C}). \tag{71c}$$

Given a vector $\boldsymbol{M}$, belonging to the material (or referential) unit sphere $\mathbb{S}^2\mathcal{B} = \{\boldsymbol{M} : \|\boldsymbol{M}\| = 1\}$, transverse isotropy with respect to the direction $\boldsymbol{M}$ is defined as the invariance under arbitrary rotations about $\boldsymbol{M}$. When the material properties do not depend on the sense of $\boldsymbol{M}$, it is possible to introduce the structure tensor $\boldsymbol{A} = \boldsymbol{M} \otimes \boldsymbol{M}$, which is invariant for inversions of $\boldsymbol{M}$, i.e. transformations of the type $\boldsymbol{M} \mapsto -\boldsymbol{M}$. For the case of transverse isotropy, two additional invariants are defined as a function of the structure tensor $\boldsymbol{A}$ [55]:

$$I_4 = \boldsymbol{C} : \boldsymbol{A} = \boldsymbol{M}\boldsymbol{C}\boldsymbol{M} = (\boldsymbol{F}\boldsymbol{M}).(\boldsymbol{F}\boldsymbol{M}) = \lambda_M^2, \tag{72a}$$

$$I_5 = \boldsymbol{C}^2 : \boldsymbol{A}, \tag{72b}$$

where λ_M^2 is the square of the stretch in direction $\boldsymbol{M}$. By enforcing the volumetric–distortional decomposition of $\boldsymbol{C}$, i.e. $\boldsymbol{C} = J^{2/3}\bar{\boldsymbol{C}}$ (see Sect. 2.1), the invariants introduced in Eqs. (71a)–(72b) can be rewritten as $I_1 = J^{2/3}\bar{I}_1$, $I_2 = J^{4/3}\bar{I}_2$, $I_3 = J^2\bar{I}_3$, $I_4 = J^{2/3}\bar{I}_4$, and $I_5 = J^{4/3}\bar{I}_5$, where the generic $\bar{I}_q$,

with $q = 1, \ldots, 5$, is obtained by substituting $\boldsymbol{C}$ with $\bar{\boldsymbol{C}}$ in the expression of the corresponding invariant I_q. Clearly, it holds that $\bar{I}_3 = \det \bar{\boldsymbol{C}} = 1$.

Appendix C. Hyperelasticity

An elastic material is called hyperelastic if the stress can be obtained by differentiation of a function, called elastic potential or elastic strain energy density, with respect to the conjugated measure of strain/deformation. If the potential is given as a function $W = \hat{W}(\boldsymbol{C})$ of the right Cauchy-Green deformation $\boldsymbol{C}$, the second Piola–Kirchhoff stress is obtained as

$$\boldsymbol{S} = 2 \frac{\partial \hat{W}}{\partial \boldsymbol{C}}(\boldsymbol{C}). \tag{73}$$

The Cauchy stress is obtained by means of the forward Piola transformation

$$\boldsymbol{\sigma} = J^{-1} \boldsymbol{F} \, \boldsymbol{S} \, \boldsymbol{F}^{\mathrm{T}} = J^{-1} \boldsymbol{F} \left[2 \frac{\partial \hat{W}}{\partial \boldsymbol{C}}(\boldsymbol{C}) \right] \boldsymbol{F}^{\mathrm{T}}. \tag{74}$$

If the material is incompressible, the kinematical constraint $J = 1$ of isochoric (i.e. volume-preserving) motion must be enforced by means of the Lagrange multiplier p (which does *not* have the physical meaning of hydrostatic pressure in this treatment), and the second Piola–Kirchhoff stress tensor is given by

$$\boldsymbol{S} = -J \, p \, \boldsymbol{B} + 2 \frac{\partial \hat{W}}{\partial \boldsymbol{C}}(\boldsymbol{C}), \tag{75}$$

where $\boldsymbol{B} = \boldsymbol{C}^{-1}$ is the Piola deformation tensor. To obtain the Cauchy stress $\boldsymbol{\sigma}$, a forward Piola transformation is performed on $\boldsymbol{S}$, i.e.

$$\boldsymbol{\sigma} = -p \, \boldsymbol{g}^{-1} + J^{-1} \boldsymbol{F} \left[2 \frac{\partial \hat{W}}{\partial \boldsymbol{C}}(\boldsymbol{C}) \right] \boldsymbol{F}^{\mathrm{T}}, \tag{76}$$

where $\boldsymbol{g}^{-1}$ is the inverse spatial metric tensor, which plays the role of the "contravariant" identity tensor.

Appendix D. Admissible interval of I_4 or $\bar{I}_4$

We want to prove that, under a deformation $\boldsymbol{C}$, the admissible values of $I_4 = \boldsymbol{C} : \boldsymbol{A}$ belong to the interval $[\lambda_{\min}^2, \lambda_{\max}^2]$, where $\lambda_{\min}^2$ and $\lambda_{\max}^2$ are the minimum and maximum eigenvalues of $\boldsymbol{C}$, for every $\boldsymbol{A} = \boldsymbol{M} \otimes \boldsymbol{M}$. The same holds for the case of the distortional part $\bar{\boldsymbol{C}}$ of the deformation, i.e. $\bar{I}_4 \in [\bar{\lambda}_{\min}^2, \bar{\lambda}_{\max}^2]$, where $\bar{\lambda}_{\min}^2$ and $\bar{\lambda}_{\max}^2$ are the minimum and maximum eigenvalues of $\bar{\boldsymbol{C}}$.

Let us consider the representation of the deformation $\boldsymbol{C}$ in terms of its eigenvalues,

$$[\boldsymbol{C}] = [C_{AB}] = \mathrm{diag}[\lambda_1^2, \ \lambda_2^2, \ \lambda_3^2], \tag{77}$$

Note that we can write the fourth invariant as

$$I_4 = \boldsymbol{C} : \boldsymbol{A} = \boldsymbol{C} : (\boldsymbol{M} \otimes \boldsymbol{M}) = \boldsymbol{M} \boldsymbol{C} \boldsymbol{M} = M^A C_{AB} M^B, \tag{78}$$

from which we obtain the equation of an ellipsoid, with matrix $[\frac{1}{I_4} C_{AB}] = \mathrm{diag}[\frac{\lambda_1^2}{I_4}, \ \frac{\lambda_2^2}{I_4}, \ \frac{\lambda_3^2}{I_4}]$, i.e.

$$M^A \left[\tfrac{1}{I_4} C_{AB} \right] M^B = 1, \quad \Rightarrow \quad \frac{(M^1)^2}{I_4/\lambda_1^2} + \frac{(M^2)^2}{I_4/\lambda_2^2} + \frac{(M^3)^2}{I_4/\lambda_3^2} = 1, \tag{79}$$

and semi-axes given by $\sqrt{I_4}/\lambda_\alpha$. If we also impose the fact that $\boldsymbol{M}$ is a unit vector, we obtain

$$\|\boldsymbol{M}\|^2 = \boldsymbol{M} . \boldsymbol{M} = \boldsymbol{M} \boldsymbol{G} \boldsymbol{M} = M^A G_{AB} M^B = 1. \tag{80}$$
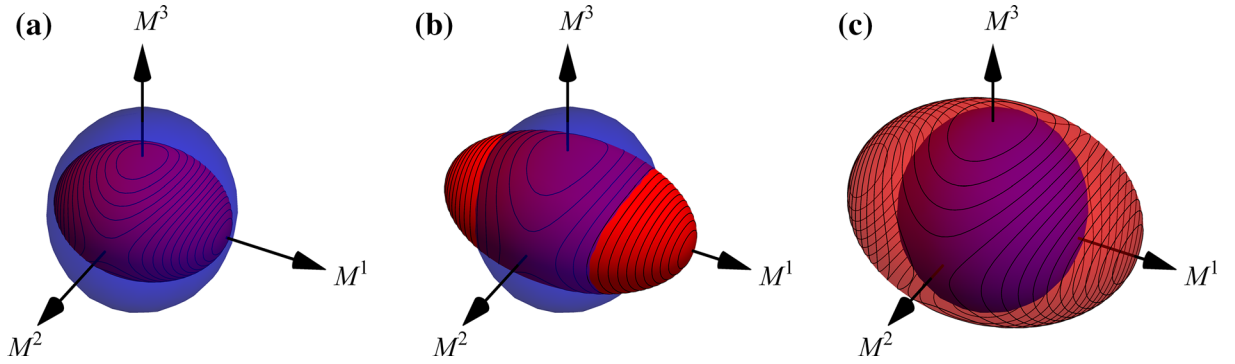
(a)   **(b)** **(c)**

FIG. 7. Graphical representation of the admissible values of I_4: **a** minimum value of I_4, **b** $I_4 \in \mathring{\Lambda}(\boldsymbol{C})$, **c** maximum value of I_4

Assuming Cartesian coordinates for simplicity of representation, we have that the matrix of the metric tensor $\boldsymbol{G}$ reduces to the identity, i.e. $G_{AB} = \delta_{AB}$, and the equation above reduces to the equation of the unit sphere

$$M^A \delta_{AB} M^B = 1, \quad \Rightarrow \quad (M^1)^2 + (M^2)^2 + (M^3)^2 = 1 \tag{81}$$

The admissible values of I_4 are those for which the ellipsoid and the sphere intersect, i.e. the system of equations given by (79) and (81) admits a solution. Evidently, the minimum value of I_4 is attained when the *major* semi-axis of the ellipsoid ($\sqrt{I_4}/\lambda_{\min}$) equals the radius of the sphere, i.e. $I_4 = \lambda^2_{\min}$ (Fig. 7a), and the maximum value of I_4 is attained when the *minor* semi-axis of the ellipsoid ($\sqrt{I_4}/\lambda_{\max}$) equals the radius of the sphere, i.e. $I_4 = \lambda^2_{\max}$ (Fig. 7c). For $I_4 \in \mathring{\Lambda}(\boldsymbol{C}) =]\lambda^2_{\min}, \lambda^2_{\max}[$, the intersection of the ellipsoid and the sphere is given by two symmetric curves (Fig. 7b).

Appendix E. Example of evaluation of the stress

In the INEX and STEX methods, our strategy for the evaluation of the stress was to first expand the ensemble potential and then differentiate the Taylor-expanded potential with respect to the deformation. This was aimed at minimising the number of integrals to be performed. As an example, let us look at the evaluation of the stress for the INEX method, in which, if the incompressibility constraint $J = 1$ is enforced, we have

$$W_e \simeq \mathcal{G}_n = \hat{\mathcal{G}}_n(\boldsymbol{C}, \Psi) = \sum_{j=0}^{n} \frac{1}{j!} \frac{\partial^{(j)} \check{W}_1}{\partial \bar{I}_4^{(j)}} (1,1) \sum_{k=0}^{j} \binom{j}{k} (-1)^k \left\langle \boldsymbol{C}^{\otimes(j-k)} \middle| \mathbb{H}_{j-k} \right\rangle. \tag{82}$$

The Cauchy stress is computed according to Eq. (76), in which $J = 1$ can be set, i.e.

$$\boldsymbol{\sigma} = \boldsymbol{F} \boldsymbol{S} \boldsymbol{F}^{\mathrm{T}} = -p\, \boldsymbol{g}^{-1} + \boldsymbol{F} \left[2 \frac{\partial \hat{W}}{\partial \boldsymbol{C}}(\boldsymbol{C}) \right] \boldsymbol{F}^{\mathrm{T}} = -p\, \boldsymbol{g}^{-1} + \boldsymbol{\sigma}_{\mathrm{c}}, \tag{83}$$

where p is the Lagrange multiplier associated with the condition $J = 1$, and $\boldsymbol{\sigma}_{\mathrm{c}}$ is the constitutive part of $\boldsymbol{\sigma}$ (here, p is not the hydrostatic pressure, because $\boldsymbol{\sigma}_{\mathrm{c}}$ need not be deviatoric in this formulation of incompressible hyperelasticity). By using the elastic potential

$$\hat{W}(\boldsymbol{C}) = \Phi_0 \hat{W}_0(\boldsymbol{C}) + \Phi_1 \int_{\mathbb{S}^2 \mathcal{B}} \Psi(\boldsymbol{M}) \hat{W}_1(\boldsymbol{C}, \boldsymbol{A}), \tag{84}$$

$\boldsymbol{\sigma}_{\mathrm{c}}$ can be written as

$$\boldsymbol{\sigma}_{\mathrm{c}} = \boldsymbol{F} \left[2\Phi_0 \frac{\partial \hat{W}_0}{\partial \boldsymbol{C}}(\boldsymbol{C}) \right] \boldsymbol{F}^{\mathrm{T}} + \boldsymbol{F} \left[2\Phi_1 \int\limits_{\mathbb{S}^2\mathcal{B}} \Psi(\boldsymbol{M}) \frac{\partial \hat{W}_1}{\partial \boldsymbol{C}}(\boldsymbol{C}, \boldsymbol{A}) \right] \boldsymbol{F}^{\mathrm{T}}$$

$$= \boldsymbol{F} \left[2\Phi_0 \frac{\partial \hat{W}_0}{\partial \boldsymbol{C}}(\boldsymbol{C}) \right] \boldsymbol{F}^{\mathrm{T}} + \boldsymbol{F} \left[2\Phi_1 \frac{\partial \hat{W}_e}{\partial \boldsymbol{C}}(\boldsymbol{C}) \right] \boldsymbol{F}^{\mathrm{T}}, \tag{85}$$

where $\hat{W}_e(\boldsymbol{C}) = \int\limits_{\mathbb{S}^2\mathcal{B}} \Psi(\boldsymbol{M})\hat{W}_1(\boldsymbol{C}, \boldsymbol{A})$ is the fibre ensemble elastic potential. Next, $\hat{W}_1(\boldsymbol{C}, \boldsymbol{A})$ is written as the sum of an isotropic and an anisotropic contribution, i.e.

$$\hat{W}_1(\boldsymbol{C}, \boldsymbol{A}) = \hat{W}_{1i}(\boldsymbol{C}) + \hat{W}_{1a}(\boldsymbol{C}, \boldsymbol{A}), \tag{86}$$

and the fibre ensemble potential becomes

$$\hat{W}_e(\boldsymbol{C}) = \hat{W}_{1i}(\boldsymbol{C}) + \int\limits_{\mathbb{S}^2\mathcal{B}} \Psi(\boldsymbol{M})\hat{W}_{1a}(\boldsymbol{C}, \boldsymbol{A}), \tag{87}$$

so that $\boldsymbol{\sigma}_{\mathrm{c}}$ takes on the form

$$\boldsymbol{\sigma}_{\mathrm{c}} = \boldsymbol{F} \left[2\Phi_0 \frac{\partial \hat{W}_0}{\partial \boldsymbol{C}}(\boldsymbol{C}) + 2\Phi_1 \frac{\partial \hat{W}_{1i}}{\partial \boldsymbol{C}}(\boldsymbol{C}) \right] \boldsymbol{F}^{\mathrm{T}} + \boldsymbol{F} \left[2\Phi_1 \int\limits_{\mathbb{S}^2\mathcal{B}} \Psi(\boldsymbol{M}) \frac{\partial \hat{W}_{1a}}{\partial \boldsymbol{C}}(\boldsymbol{C}, \boldsymbol{A}) \right] \boldsymbol{F}^{\mathrm{T}}. \tag{88}$$

The general formula (88) should now be specialised according to the approximation method that is adopted. Since both $\hat{W}_0(\boldsymbol{C})$ and $\hat{W}_{1i}(\boldsymbol{C})$ contribute to $\boldsymbol{\sigma}_{\mathrm{c}}$ in the same way for all methods (indeed, they are independent of the direction of the fibres and thus need not be approximated by any of our methods), we can restrict our calculations by focusing on the anisotropic stress contribution of the fibres only, i.e.

$$\boldsymbol{\sigma}_{1a} := \boldsymbol{F} \left[2\Phi_1 \int\limits_{\mathbb{S}^2\mathcal{B}} \Psi(\boldsymbol{M}) \frac{\partial \hat{W}_{1a}}{\partial \boldsymbol{C}}(\boldsymbol{C}, \boldsymbol{A}) \right] \boldsymbol{F}^{\mathrm{T}}. \tag{89}$$

Moreover, since the averaging integral in (89) pertains only to the partial second Piola–Kirchhoff stress tensor

$$\boldsymbol{S}_{1a} := 2\Phi_1 \int\limits_{\mathbb{S}^2\mathcal{B}} \Psi(\boldsymbol{M}) \frac{\partial \hat{W}_{1a}}{\partial \boldsymbol{C}}(\boldsymbol{C}, \boldsymbol{A}), \tag{90}$$

it suffices for our purposes to provide, for each of the four proposed approximation methods, the corresponding approximated expression of $\boldsymbol{S}_{1a}$, which we denote by $\boldsymbol{S}_{1a}^{\mathrm{app}}$. The stress $\boldsymbol{S}_{1a}$ computed according to the FESDH method shall be regarded as "exact".

We recall that, for the FESDH method, $\hat{W}_{1a}(\boldsymbol{C}, \boldsymbol{A}) = \mathcal{H}(\boldsymbol{C} : \boldsymbol{A} - 1)\hat{W}_{1b}(\boldsymbol{C}, \boldsymbol{A})$, and $\boldsymbol{S}_{1a}$ is given by

$$\boldsymbol{S}_{1a} = 2\Phi_1 \int\limits_{\mathbb{S}^2\mathcal{B}} \Psi(\boldsymbol{M})\mathcal{H}(\boldsymbol{C} : \boldsymbol{A} - 1) \frac{\partial \hat{W}_{1b}}{\partial \boldsymbol{C}}(\boldsymbol{C}, \boldsymbol{A}). \tag{91}$$

In the FESD, INEX, PARG and STEX methods, we do not premultiply $\hat{W}_{1b}$ by the Heaviside function, so that $\hat{W}_{1a}(\boldsymbol{C}, \boldsymbol{A}) \equiv \hat{W}_{1b}(\boldsymbol{C}, \boldsymbol{A})$ holds true. Thus, with reference to the FESD approximation, $\boldsymbol{S}_{1a}^{\mathrm{app}}$ is given by

$$\boldsymbol{S}_{1a}^{\mathrm{app}} = 2\Phi_1 \int\limits_{\mathbb{S}^2\mathcal{B}} \Psi(\boldsymbol{M}) \frac{\partial \hat{W}_{1a}}{\partial \boldsymbol{C}}(\boldsymbol{C}, \boldsymbol{A}) = 2\Phi_1 \frac{\partial}{\partial \boldsymbol{C}} \int\limits_{\mathbb{S}^2\mathcal{B}} \Psi(\boldsymbol{M})\hat{W}_{1a}(\boldsymbol{C}, \boldsymbol{A}). \tag{92}$$

For the INEX method, we approximate $\int_{\mathbb{S}^2\mathcal{B}} \Psi(\boldsymbol{M})\hat{W}_{1a}(\boldsymbol{C}, \boldsymbol{A})$ as

$$\int_{\mathbb{S}^2\mathcal{B}} \Psi(\boldsymbol{M})\hat{W}_{1a}(\boldsymbol{C}, \boldsymbol{A}) \simeq \sum_{j=0}^{n} \frac{1}{j!} \frac{\partial^{(j)}\check{W}_{1a}}{\partial \bar{I}_4^{(j)}}(1,1) \sum_{k=0}^{j} \binom{j}{k}(-1)^k \left\langle \boldsymbol{C}^{\otimes(j-k)} \middle| \mathbb{H}_{j-k} \right\rangle. \tag{93}$$

Consequently, $\boldsymbol{S}_{1a}^{\mathrm{app}}$ reads

$$\boldsymbol{S}_{1a}^{\mathrm{app}} = 2\Phi_1 \sum_{j=1}^{n} \frac{1}{j!} \frac{\partial^{(j)}\check{W}_{1a}}{\partial \bar{I}_4^{(j)}}(1,1) \sum_{k=0}^{j-1} \binom{j}{k}(-1)^k \frac{\partial}{\partial \boldsymbol{C}} \left\langle \boldsymbol{C}^{\otimes(j-k)} \middle| \mathbb{H}_{j-k} \right\rangle, \tag{94}$$

and one has to compute the derivative

$$\boldsymbol{T} : \left(\frac{\partial}{\partial \boldsymbol{C}} \left\langle \boldsymbol{C}^{\otimes\ell} \middle| \mathbb{H}_\ell \right\rangle \right) = \ell \left\langle \mathbb{H}_\ell \middle| \boldsymbol{T} \otimes \boldsymbol{C}^{\otimes(\ell-1)} \right\rangle, \quad \ell \in \mathbb{N}, \ \ell \geq 1, \ n \geq 1, \tag{95}$$

where $\boldsymbol{T}$ is an arbitrary "covariant" second-order tensor. This result can be proven by invoking the fact that, at least in the case of transverse isotropy, $\mathbb{H}_\ell$ is fully symmetric for every ℓ, and noticing that (we show the explicit index calculation only for $\ell = 1, 2$):

$$\frac{\partial}{\partial C_{RS}} \left\langle \boldsymbol{C}^{\otimes 1} \middle| \mathbb{H}_1 \right\rangle = \frac{\partial}{\partial C_{RS}} \left(C_{MN}(\mathbb{H}_1)^{MN} \right) = (\mathbb{I}^{\mathrm{T}})_{MN}{}^{RS}(\mathbb{H}_1)^{MN} = (\mathbb{H}_1)^{RS}, \tag{96}$$

$$\frac{\partial}{\partial C_{RS}} \left\langle \boldsymbol{C}^{\otimes 2} \middle| \mathbb{H}_2 \right\rangle = \frac{\partial}{\partial C_{RS}} \left(C_{MN} C_{PQ}(\mathbb{H}_2)^{MNPQ} \right)$$

$$= (\mathbb{I}^{\mathrm{T}})_{MN}{}^{RS} C_{PQ}(\mathbb{H}_2)^{MNPQ} + C_{MN}(\mathbb{I}^{\mathrm{T}})_{PQ}{}^{RS}(\mathbb{H}_2)^{MNPQ}$$

$$= 2(\mathbb{H}_2)^{RSAB} C_{AB}. \tag{97}$$

Therefore, we obtain (again with the help of an arbitrary "covariant" second-order tensor $\boldsymbol{T}$)

$$\boldsymbol{T} : \boldsymbol{S}_{1a}^{\mathrm{app}} = 2\Phi_1 \sum_{j=1}^{n} \frac{1}{j!} \frac{\partial^{(j)}\check{W}_{1a}}{\partial \bar{I}_4^{(j)}}(1,1) \sum_{k=0}^{j-1} \binom{j}{k}(-1)^k (j-k) \left\langle \mathbb{H}_{j-k} \middle| \boldsymbol{T} \otimes \boldsymbol{C}^{\otimes(j-k-1)} \right\rangle. \tag{98}$$

For the PARG method, we write $\hat{W}_{1a}(\boldsymbol{C}, \boldsymbol{A}) = \mathfrak{f}(\mathcal{P}(\boldsymbol{C}, \boldsymbol{A}))$, where $\mathfrak{f}$ is any differentiable function of its argument, and $\mathcal{P}(\boldsymbol{C}, \boldsymbol{A})$ is a tensor-power polynomial. Then, we enforce the approximation

$$\int_{\mathbb{S}^2\mathcal{B}} \Psi(\boldsymbol{M})\hat{W}_{1a}(\boldsymbol{C}, \boldsymbol{A}) = \int_{\mathbb{S}^2\mathcal{B}} \Psi(\boldsymbol{M})\mathfrak{f}(\mathcal{P}(\boldsymbol{C}, \boldsymbol{A})) \simeq \mathfrak{f}\left(\int_{\mathbb{S}^2\mathcal{B}} \Psi(\boldsymbol{M})\mathcal{P}(\boldsymbol{C}, \boldsymbol{A}) \right). \tag{99}$$

and $\boldsymbol{S}_{1a}^{\mathrm{app}}$ becomes

$$\boldsymbol{S}_{1a}^{\mathrm{app}} = 2\,\Phi_1\,\mathfrak{f}'\left(\int_{\mathbb{S}^2\mathcal{B}} \Psi(\boldsymbol{M})\mathcal{P}(\boldsymbol{C}, \boldsymbol{A}) \right) \left(\frac{\partial}{\partial \boldsymbol{C}} \int_{\mathbb{S}^2\mathcal{B}} \Psi(\boldsymbol{M})\mathcal{P}(\boldsymbol{C}, \boldsymbol{A}) \right). \tag{100}$$

In the specific case in which

$$\mathfrak{f}(\mathcal{P}(\boldsymbol{C}, \boldsymbol{A})) = \tfrac{1}{2}c_{1a}\left[\exp\left(\mathcal{P}(\boldsymbol{C}, \boldsymbol{A})\right) - 1 \right] \text{ and } \mathcal{P}(\boldsymbol{C}, \boldsymbol{A}) = (\langle \boldsymbol{C} | \boldsymbol{A} \rangle - 1)^2,$$

so that

$$\int_{\mathbb{S}^2\mathcal{B}} \Psi(\boldsymbol{M})\mathcal{P}(\boldsymbol{C}, \boldsymbol{A}) = \langle \boldsymbol{C}^{\otimes 2} | \mathbb{H}_2 \rangle - 2\langle \boldsymbol{C} | \mathbb{H}_1 \rangle + 1, \tag{101}$$

we obtain

$$
\boldsymbol{S}_{1a}^{\mathrm{app}} = \Phi_1 c_{1a} \exp\left(\int\limits_{\mathbb{S}^2 \mathcal{B}} \Psi(\boldsymbol{M})\mathcal{P}(\boldsymbol{C},\boldsymbol{A})\right)\left(\frac{\partial}{\partial \boldsymbol{C}}\int\limits_{\mathbb{S}^2 \mathcal{B}} \Psi(\boldsymbol{M})\mathcal{P}(\boldsymbol{C},\boldsymbol{A})\right)
$$
$$
= \Phi_1 c_{1a} \exp\left(\langle \boldsymbol{C}^{\otimes 2}|\mathbb{H}_2\rangle - 2\langle \boldsymbol{C}|\mathbb{H}_1\rangle + 1\right)(2\mathbb{H}_2 : \boldsymbol{C} - 2\mathbb{H}_1). \tag{102}
$$

Finally, for the STEX method, if $\boldsymbol{T}$ is an arbitrary "covariant" second-order tensor, we have

$$
\boldsymbol{T} : \boldsymbol{S}_{1a}^{\mathrm{app}} = \boldsymbol{T} : 2\Phi_1 \frac{\partial \hat{W}_{1a}}{\partial \boldsymbol{C}}(\boldsymbol{C},\boldsymbol{A})
$$
$$
+ 2\Phi_1 \sum_{j=1}^{n}\left\langle \frac{1}{j!}\frac{\partial^{(j+1)}\hat{W}_{1a}}{\partial \boldsymbol{A}^{(j)}\partial \boldsymbol{C}}(\boldsymbol{C},\boldsymbol{A}_0)\,\middle|\,\boldsymbol{T} \otimes \sum_{k=0}^{j}\left[(-1)^k \binom{j}{k}\mathrm{msym}\left(\mathbb{H}_{j-k} \otimes \boldsymbol{A}_0^{\otimes k}\right)\right]\right\rangle. \tag{103}
$$

References

1. Fung, Y.C.: Biomechanics. Motion, Flow, Stress, and Growth. Springer, New York (1990)
2. Bachrach, N.M., Mow, V.C., Guilak, F.: Incompressibility of the solid matrix of articular cartilage under high hydrostatic pressures. J. Biomech. **31**, 445–451 (1998)
3. El Nady, K., Ganghoffer, J.F.: Computation of the effective mechanical response of biological networks accounting for large configuration changes. J. Mech. Behav. Biol. Mater. **58**, 28–44 (2016)
4. Butler, D.L., Grood, E.S., Noyes, F.R., Zernicke, R.E.: Biomechanics of ligaments and tendons. Exerc. Sport Sci. Rev. **6**(1), 125–182 (1978)
5. Holzapfel, G.A., Gasser, T.C., Ogden, R.W.: A new constitutive framework for arterial wall mechanics and a comparative study of material models. J. Elast. **61**, 1–48 (2000)
6. Gasser, T.C., Ogden, R.W., Holzapfel, G.A.: Hyperelastic modelling of arterial layers with distributed collagen fibre orientations. J. R. Soc. Interface **3**, 15–35 (2006)
7. Bellini, C., Di Martino, E.S.: A mechanical characterization of the porcine atria at the healthy stage and after ventricular tachypacing. J. Biomech. Eng. **134**, 021008 (2012)
8. Bellini, C., Di Martino, E.S., Federico, S.: Mechanical behaviour of the human atria. Ann. Biomed. Eng. **41**, 1478–1490 (2013)
9. Aspden, R.M., Hukins, D.W.L.: Collagen organization in articular cartilage, determined by X-ray diffraction, and its relationship to tissue function. Proc. R. Soc. Lond. Ser. B **212**, 299–304 (1981)
10. Mollenhauer, J., Aurich, M., Muehleman, C., Khelashvili, G., Irving, T.C.: X-ray diffraction of the molecular substructure of human articular cartilage. Connect. Tissue Res. **44**, 201–207 (2003)
11. Lanir, Y.: Constitutive equations for fibrous connective tissues. J. Biomech. **16**, 1–12 (1983)
12. Hurschler, C., Loitz-Ramage, B., Vanderby, R. Jr.: A structurally based stress–stretch relationship for tendon and ligament. J. Biomech. Eng. **119**, 392–399 (1997)
13. Billiar, K.L., Sacks, M.S.: Biaxial mechanical properties of the native and glutaraldehyde-treated aortic valve cusp: part II—a structural constitutive model. J. Biomech. Eng. **122**, 327–335 (2000)
14. Sacks, M.S.: Incorporation of experimentally-derived fiber orientation into a structural constitutive model for planar collagenous tissues. J. Biomech. Eng. **125**, 280–287 (2003)
15. Federico, S., Grillo, A., Herzog, W.: A transversely isotropic composite with a statistical distribution of spheroidal inclusions: a geometrical approach to overall properties. J. Mech. Phys. Solids **52**, 2309–2327 (2004)
16. Federico, S., Herzog, W.: On the permeability of fibre-reinforced porous materials. Int. J. Solids Struct. **45**, 2160–2172 (2008)
17. Federico, S., Herzog, W.: Towards an analytical model of soft tissues. J. Biomech. **41**, 3309–3313 (2008)
18. Federico, S., Grillo, A.: Elasticity and permeability of porous fibre-reinforced materials under large deformations. Mech. Mater. **44**, 58–71 (2012)
19. Federico, S.: Porous materials with statistically oriented reinforcing fibres. In: Dorfmann, L., Ogden, R.W. (eds.) In Nonlinear Mechanics of Soft Fibrous Materials, CISM Courses and Lectures No. 559, International Centre for Mechanical Sciences. Springer, Berlin (2015)
20. Federico, S., Gasser, T.G.: Non-linear elasticity of biological tissues with statistical fibre orientation. J. R. Soc. Interface **7**, 955–966 (2010)

21. Hardin, R.H., Sloane, N.J.A.: McLaren's improved snub cube and other new spherical designs in three dimensions. Discret. Comput. Geom. **15**, 429–441 (1996)
22. Lebedev, V.I.: Quadratures on a sphere. USSR Comput. Math. Math. Phys. **16**, 10–24 (1976)
23. Bažant, P., Oh, B.H.: Efficient numerical integration on the surface of a sphere. Zeitschrift für Angewandte Mathematik Und Mechanik (J. Appl. Math. Mech.) **66**, 37–49 (1986)
24. Heo, S.-W., Xu, Y.: Constructing fully symmetric cubature formulae for the sphere. Math. Comput. **70**(233), 269–279 (2001)
25. Skacel, P., Bursa, J.: Numerical implementation of constitutive model for arterial layers with distributed collagen fibre orientations. Comput. Methods Biomech. Biomed. Eng. **18**, 816–828 (2015)
26. Carfagna, M., Grillo, A.: The spherical design algorithm in the numerical simulation of biological tissues with statistical fibre-reinforcement (submitted)
27. Flory, P.J.: Thermodynamic relations for high elastic materials. Trans. Faraday Soc. **57**, 829–838 (1961)
28. Ogden, R.W.: Nearly isochoric elastic deformations: application to rubberlike solids. J. Mech. Phys. Solids **26**, 37–57 (1978)
29. Ogden, R.W.: Non-linear Elastic Deformations. Dover, New York (1997)
30. Kanatani, K.: Stereological determination of structural anisotropy. Int. J. Eng. Sci. **22**, 531–546 (1984)
31. Advani, S.G., Tucker, C.L.: The use of tensors to describe and predict fiber orientation in short fiber composites. J. Rheol. **31**, 751–784 (1987)
32. Epstein, M.: The Geometrical Language of Continuum Mechanics. Cambridge University Press, Cambridge (2010)
33. Segev, R.: Notes on metric independent analysis of classical fields. Math. Methods Appl. Sci. **36**, 497–566 (2013)
34. Hardin, R.H., Sloane, N.J.A., Smith, W.D.: Spherical Codes (2008). http://www.research.att.com/~njas/packings/
35. Lanir, Y., Namani, R.: Reliability of structure tensors in representing soft tissues structure. J. Mech. Behav. Biomed. Mater. **46**, 222–228 (2015)
36. Walpole, L.J.: Elastic behavior of composite materials: theoretical foundations. Adv. Appl. Mech. **21**, 169–242 (1981)
37. Walpole, L.J.: Fourth-rank tensors of the thirty-two crystal classes: multiplication tables. Proc. R. Soc. Lond. Ser. A **391**, 149–179 (1984)
38. Vasta, M., Gizzi, A., Pandolfi, A.: On three- and two-dimensional fiber distributed models of biological tissues. Probab. Eng. Mech. **37**, 170–179 (2014)
39. Gizzi, A., Pandolfi, A., Vasta, M.: Statistical characterization of the anisotropic strain energy in soft materials with distributed fibers. Mech. Mater. **92**, 119–138 (2016)
40. Römgens, A.M., van Donkelaar, C.C., Ito, K.: Contribution of collagen fibers to the compressive stiffness of cartilaginous tissues. Biomech. Model. Mechanobiol. **12**, 1221–1231 (2013)
41. Mansour, J.M.: Biomechanics of cartilage. In: Oatis, C.A. (ed.) In Kinesiology: The Mechanics and Pathomechanics of Human Movement. 2nd edn, pp. 69–83. Lippincott Williams & Wilkins, Philadelphia (2009)
42. Fratzl, P., Misof, K., Zizak, I., Rapp, G., Amenitsch, H., Bernstorff, S.: Fibrillar structure and mechanical properties of collagen. J. Struct. Biol. **112**, 119–122 (1997)
43. Destrade, M., Mac Donald, B., Murphy, J.G., Saccomandi, G.: At least three invariants are necessary to model the mechanical response of in-compressible, transversely isotropic materials. Comput. Mech. **52**, 959–969 (2013)
44. Fung, Y.C.: Elasticity of soft tissues in simple elongation. Am. J. Physiol. **213**, 1532–1544 (1967)
45. Wilber, J.P., Walton, J.R.: The convexity properties of a class of constitutive models for biological soft tissues. Math. Mech. Solids **7**, 217–235 (2002)
46. Humphrey, J.D.: Continuum biomechanics of soft biological tissues. Proc. R. Soc. Lond. Ser. A **459**, 1–44 (2003)
47. Federico, S., Grillo, A., Giaquinta, G., Herzog, W.: Convex Fung-type potentials for biological tissues. Meccanica **43**, 279–288 (2008)
48. Tomic, A., Grillo, A., Federico, S.: Poroelastic materials reinforced by statistically oriented fibres—numerical implementation and application to articular cartilage. IMA J. Appl. Math. **79**, 1027–1059 (2014)
49. Weisstein, E.W.: Erfi. From MathWorld—A Wolfram Web Resource (2005). http://mathworld.wolfram.com/Erfi.html
50. Pajerski, J.: Nonlinear Biphasic Microstructural Numerical Analysis of Articular Cartilage and Chondrocytes. MSc Thesis, The University of Calgary, Canada (2010)
51. dell'Isola, F., Steigmann, D.J.: A two-dimensional gradient-elasticity theory for woven fabrics. J. Elast. **118**, 113–125 (2015)
52. Steigmann, D.J., dell'Isola, F.: Mechanical response of fabric sheets to three-dimensional bending, twisting, and stretching. Acta Mech. Sin. **31**, 373–382 (2015)
53. Giorgio, I., Grygoruk, R., dell'Isola, F., Steigmann, D.J.: Pattern formation in the three-dimensional deformations of fibered sheets. Res. Mech. Commun. **69**, 164–171 (2015)
54. Eringen, A.C.: Mechanics of Continua. Robert E. Krieger Publishing Company, Huntington (1980)
55. Spencer, A.J.M.: Constitutive theory for strongly anisotropic solids. In: Spencer, A.J.M. (ed.) Continuum Theory of the Mechanics of Fibre-Reinforced Composites, CISM Courses and Lectures No. 282, International Centre for Mechanical Sciences, pp. 1–32. Springer, Wien (1984)

Kotaybah Hashlamoun
Graduate Programme in Mechanical Engineering
The University of Calgary
2500 University Drive NW
Calgary, AB, T2N 1N4, Canada

Alfio Grillo
DISMA - Department of Mathematical Sciences "G.L. Lagrange"
Politecnico di Torino
Corso Duca degli Abruzzi 24
10124, Turin, Italy

Salvatore Federico
Department of Mechanical and Manufacturing Engineering
The University of Calgary
2500 University Drive NW
Calgary, AB, T2N 1N4, Canada
e-mail: salvatore.federico@ucalgary.ca